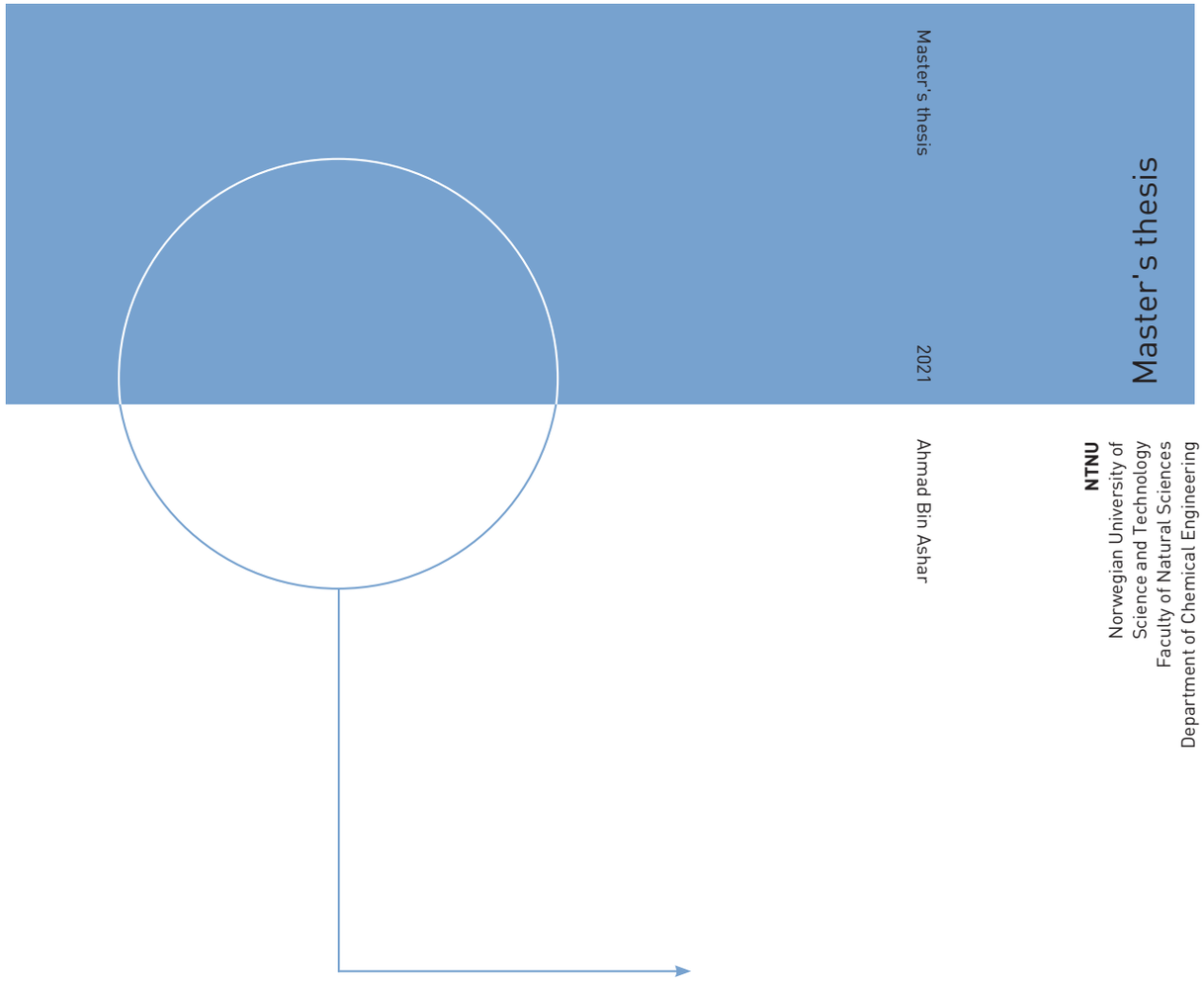

Ahmad Bin Ashar

Magnetic Polymeric Nanoparticles for Biomedical Applications

February 2021

NTNU
Norwegian University of
Science and Technology

NTNU
Norwegian University of
Science and Technology

NTNU

Norwegian University of
Science and Technology

Magnetic Polymeric Nanoparticles for Biomedical Applications

Ahmad Bin Ashar

Master's in Chemical Engineering
Submission date: February 2021
Supervisor: Sulalit Bandyopadhyay
Co-supervisor: Anuvansh Sharma

Norwegian University of Science and Technology
Department of Chemical Engineering

Declaration of Compliance

I, Ahmad Bin Ashar, hereby declare that this is an independent work according to the exam regulations of Norwegian University of Science and Technology (NTNU).

Place and Date: Trondheim – Gløshaugen, February 2021

Acknowledgement

First and foremost, I would love to thank my supervisor **Dr. Sulalit Bandyopadhyay** for his excellent supervision and unforgettable support during my master thesis. Being with **Dr. Sulalit**, I have earned valuable research and interpersonal skills that would be essential in all aspects of my career as a researcher. His devotion and motivation in research has always inspired me and has been a driving force for me to excel in field of nanomaterials. I would also like to pay my gratitude to my Co-Supervisor **Anuvansh Sharma** for his availability for research discussion.

The fellows of Particle Engineering Research Group have always actively helped me in improving my research capabilities with healthy discussions during the group meetings. They have always provided a friendly working environment.

I would also thank my parents especially my father who has always groomed and preached me as mentor and my loving wife for their moral support throughout my master's degree.

My friends, Hammad Farooq and Zeeshan Ali has provided the best company during work and after.

At last, I thank **Allah Almighty** for showering his countless blessings and providing me an opportunity to study and work in NTNU.

Abstract

Iron Oxide Nanoparticles (IONPs) have been extensively used in different applications including biomedicine, hydrology, and catalysis. This is because IONPs have excellent physico-chemical properties like superparamagnetism. These IONPs can be encapsulated into various polymers using different techniques like emulsion-diffusion, salting out, and nanoprecipitation whereby increasing their applicability in various fields.

Many researchers have investigated the encapsulation of hydrophobic moieties into polymers by the using the technique of nanoprecipitation but very few research papers have been published where hydrophilic moieties are encapsulated into polymers by the above-mentioned technique. The aim of this project was to encapsulate the hydrophilic moieties i.e., IONPs into different polymers by using nanoprecipitation.

In this master thesis, firstly IONPs and bare polymeric NPs of PLGA were synthesized using the technique of co-precipitation and nanoprecipitation, respectively in section 4.1. Secondly, IONPs were then encapsulated by PLGA NPs using the technique of nanoprecipitation. This encapsulation process was optimized via different methodology which are briefly discussed in section 4.2. Thirdly, the study of different parameters like polymer amount, amount of IONPs, Aqueous/Organic ratio and injection rate that can influence the PLGA encapsulated IONPs size was performed using a statistical software i.e., JMP in section 4.3. Finally, in the last section 4.4, bare PLGA NPs and PLGA encapsulated IONPs were loading with a hydrophobic drug i.e., coumarin. The IONPs were characterized using High Resolution Transmission Electron Microscopy (HRTEM), PLGA encapsulated IONPs were characterized using Dynamic Light Scattering (DLS) and drug loading efficiency was estimated using Ultra Violet Visible Spectroscopy (UV-Vis).

The IONPs synthesized by co-precipitation method had polydisperse population with an average diameter of 15 ± 2 nm. The hydrodynamic size of PLGA NPs before encapsulation with the IONPs was in the range of 80-110 nm. After encapsulation of the IONPs with PLGA NPs, the hydrodynamic size was obtained in the range from 400-800 nm. The process of encapsulation of IONPs with PLGA NPs was successfully

optimized using different methodologies. The JMP design for study of different parameters was performed using screening design. In screening design, backward selection of the least significant variable in the data set is done. Because the least significant variable has the maximum effect on the data set. In the first JMP design, Fe/Polymer ratio and molecular weight of polymer were the least significant variables. In the second JMP study, molecular weight, and amount of IONPs were found to be the least significant variables. In the last study, coumarin was loaded in PLGA NPs and PLGA encapsulated IONPs. The drug loading efficiency for bare PLGA NPs was found to be around 92 % and for PLGA encapsulated IONPs it was around 90 % when highest amount of drug was used. Hence, in this project, successful encapsulation of IONPs (hydrophilic moieties) and drug loading of coumarin in PLGA encapsulated IONPs was achieved by the technique of nanoprecipitation which has not been reported in the literature until date.

Table of Contents

List of Figures

List of Tables

List of Abbreviations

IONPs	Iron Oxide Nanoparticles
PLGA	Poly (lactide-co-glycolide) acid
PNPs	Polymeric Nanoparticles
NPs	Nanoparticles
PLGA-MAG NPs	PLGA encapsulated IONPs

1. Introduction

This chapter starts with an introduction to Iron Oxide Nanoparticles (IONPs) where their physico-chemical properties are discussed. After IONPs introduction, a brief overview of polymers is presented in section 1.2. Following that, an introduction to Poly(lactide-co-glycolide) acid (PLGA), physico-chemical properties of PLGA and synthesis of PLGA are discussed in detail. In section 1.3, different techniques to synthesize polymeric NPs are highlighted. Section 1.4 contains an introduction of nanoprecipitation, a detailed discussion of mechanism of nanoprecipitation in the light of literature, and study of important parameters that can affect the NPs size in nanoprecipitation. In the final section, applications of PLGA NPs and PLGA encapsulated IONPs (mentioned as PLGA-MAG NPs in this whole report) are discussed briefly.

1.1 Iron Oxide Nanoparticles (IONPs)

Iron oxide Nanoparticles (IONPs), due to their physiochemical properties like superparamagnetism have been employed in different applications including targeted drug delivery, catalysis, hyperthermia, and magnetic response imaging (MRI) etc. Superparamagnetism is a type of magnetism, present in ferromagnetic or ferrimagnetic NPs. Under the influence of temperature, the domains of NPs due to magnetization flip direction randomly. The time interval between two flips is called Neel relaxation time. If the time of magnetization measurement for NPs is longer than Neel relaxation time, in the absence of external magnetic field, then the average value of magnetization of NPs is almost zero. Such NPs are in superparamagnetic state.[1] For NPs to be superparamagnetic, they should be constituted of single magnetic domains i.e., each atom of NPs should be a single magnetic domain. During magnetization, the NPs will have a single big magnetic moment. Possibility of NPs to be superparamagnetic is when they have diameter below 3-50 nm.[1]

IONPs can be synthesized using various synthesis techniques like co-precipitation, thermal decomposition, hydrothermal synthesis, and sol-gel synthesis etc. In synthesis technique like thermal decomposition, IONPs are mostly synthesized in organic solvents and are needed to be phase

transferred into water for most of their applications specially in biomedicine. Phase transfer of IONPs also helps in prevention of aggregation and improvement of colloidal stability. In most of the surface modification processes, the hydrophobic surface of IONPs is modified with a polymer or a ligand which is hydrophilic and promotes the stability of IONPs in aqueous phase. IONPs can be sterically stabilized by embedding a polymer or ligand shell.[2] Electrostatic stabilization of IONPs is achieved by adsorption of ions of stabilizers on the surface of IONPs e.g. sodium citrate acts as a very good stabilizer and the citrate anions are adsorbed on the surface of IONPs to provide electrostatic stability and hence IONPs become colloidally stable.[3] Other examples of phase transfer ligands are citric acid [4], Pluronic F127 [5], α-cyclodextrin [6], polyethylene glycol (PEG) [7] and Chitosan [8], they alter the hydrophobic nature of IONPs into hydrophilic nature and prevents aggregation of IONPs.

Monodispersity of IONPs is important for biomedical and other applications because if the IONPs are aggregated then there is a variation in the magnetic properties of IONPs which makes it difficult to use them for their further applications. For instance, if they are used for hyperthermia, the alternating magnetic field induced heating is highly affected by aggregation. [9]

For applications like targeted drug delivery, IONPs are encapsulated into polymers using different techniques namely nanoprecipitation, emulsion-diffusion, salting-out, flash nanoprecipitation and solvent evaporation etc. Encapsulation of IONPs along with specific drugs is important in order to protect the NPs from aggregation and chemical degradation. The main purpose of encapsulating IONPs into polymer matrix along with drug is to utilize their magnetic properties for targeted drug delivery. The applications of polymer encapsulated IONPs will be discussed in detail in section 1.5.

In the upcoming section polymers will be discussed in detail including biodegradable polymers like PLGA. Their physico-chemical properties and synthesis procedures will be highlighted.

1.2 Polymers

Polymers are macromolecules which are made up of small units called monomers. They are found in nature as proteins, nucleic acids, natural rubber, wool etc. In 1830s, the first man-made polymer synthesis procedure for derivates of cellulose like celluloid and cellulose acetate was developed by Henri Braconnots in collaboration with Christian Schönbein and others.[10] Synthetic plastics and fibres industries flourished a lot until 1960s but due to non-biodegradability and environmental concerns of these polymers, scientists started looking into biodegradable and bio-compatible polymers.

In 1962, first synthetic biodegradable polymer polyglycolic acid (PGA) was synthesized by American Cyanamid Co.[11] The company developed absorbable sutures named Dexton and these sutures were commercially available since 1970s. Within a decade, an extensive research started on biodegradable polymers like polylactic acid (PLA), polyglycolic acid (PGA), polylactic-co-glycolic acid (PLGA), polycaprolactone (PCL) etc owing to their diverse applications in dentistry, drug delivery, orthopaedic, and bone tissue engineering etc.[11-13]

Due to the biodegradability of above-mentioned polymers, after 1970s, researchers started investigating these polymers for different biomedical applications such as cancer treatment etc. The most commonly used polymer for drug delivery systems is PLGA. This polymer has now been extensively used as a drug carrier by making NPs of PLGA and loading them with various drugs such as ibuprofen [14], doxorubicin [15] and paracetamol [16] etc. The drug delivery occurs after the degradation and erosion of polymeric shell in response to external stimuli such as temperature and pH etc. [17] The synthesis of PLGA NPs and the applications of PLGA NPs in biomedicine will be discussed in more detail in upcoming sections.

1.2.1 Poly(lactide-co-glycolide) acid (PLGA)

One of the most commonly used biocompatible and biodegradable polymer in drug delivery and tissue engineering, is PLGA. PLGA is a Food and Drug Administration (FDA) approved polymer which means it can be used in biomedicine without any further approval and hence its

medicinal applications can be transferred easily to mankind. Above all, this polymer can be transformed into small NPs which can then encapsulate drug molecules and can be used for various disease treatments such as cancer. The drug delivery applications of PLGA NPs are discussed in detail in section 1.5. The reason for polymeric particles to be in nanometre range is probably because if they are bigger than 200 nm, they will be detected by the mononuclear phagocyte system (MPS) and reticuloendothelial system (RES) in the blood stream and would not be able to reach the targeted drug delivery area. [18] Hence, their size and surface properties must be tuned in such a way that they reach the targeted area in the body. In the next section physicochemical properties of PLGA will be discussed briefly which have a vital impact on its applicability in biomedical applications.

1.2.1.1 Physicochemical Properties of PLGA

PLGA is composed of repeating units of lactic and glycolic acid. It can be synthesized by two synthesis methods. First is by direct polycondensation of lactide and glycolide to form low molecular weight and broadly molar mass distributed PLGA. Second is by ring opening polymerization of lactide and glycolide to obtain high molecular weight and narrowly molar mass distributed PLGA. The molecular weight of PLGA can be adjusted from 4 to 240 kDa by varying the polymerization conditions or by adjusting the ratios of monomer and initiator. [19]

Various factors such as composition and molecular weight can affect the biodegradation rate of PLGA. The degradation rate is predominantly dependant on the ratio of glycolide units, since these units have hydrophilic nature, and they are more susceptible to hydrolysis. The degradation in PLGA happens in four consecutive steps i.e., hydration, initial degradation, further degradation and solubilization. In the first step, water enters the polymer structure and causes the relaxation of polymer and decrease in glass transition temperature (T_g). In second step, the degradation occurs via ester bond hydrolysis resulting in lowering of molecular weight and cleavage of polymer backbone. The second step continues until the mechanical strength of polymer is not lost but the polymer is still integrated. In third step, the polymer chains break and the molecular weight declines to a point where the polymer cannot keep itself

integrated and it starts to lose its mass. In final step, the polymer units are further converted into molecules which are soluble in water. [20]

Studies in literature has shown that PLGA with 50:50 ratio of lactide and glycolide groups which degrade faster relative to ratios like 65:35 and 75:25 etc. Hence due to this reason they are more commonly used in biomedicine.[21] PLGA can also undergo bulk degradation in an aqueous medium meaning that hydration rate is faster than polymer solubilization.[22] A schematic of hydrolysis of PLGA is presented as follows:

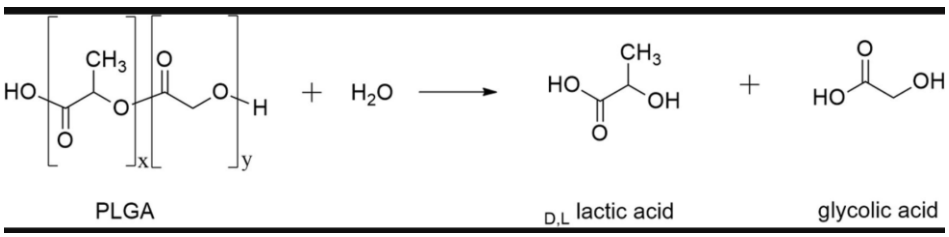

Figure 1: PLGA degradation into D, L-lactic acid, and glycolic acid due to hydrolysis [23]

The degradation of PLGA is an important property that can greatly influence the drug release. If the degradation is very slow, then the drug would be released slowly, and drug release efficiency will not be good as well.

Dissolution of PLGA in different organic solvents is also dependent on its composition (LA/GA ratio). If the ratio of LA is more than GA group in PLGA then, this polymer is dissolved in chlorinated solvents like dichloromethane and chloroform and also in water-miscible solvents such as acetone and tetrahydrofuran etc. While fluorinated solvents like hexafluoro isopropanol are preferred if the GA ratio is more than LA groups in PLGA. [23]

The glass transition temperature of PLGA ranges between 40 and 60 ºC which is above human body temperature. It can be altered by decreasing

the molecular weight of the polymer or by decreasing the lactide ratio in PLGA.

In the next section synthesis of PLGA via different routes will be discussed in detail in the light of literature.

1.2.1.2 Synthesis of PLGA

PLGA can be synthesized by direct polycondensation or ring opening polymerization of lactide and glycolide. Here in this section both of the methods will be discussed briefly with references from the literature.

PLGA synthesized by direct polycondensation yields polymer with low molecular weight (Mw < 10 kDa). Zhou et al.[24] synthesized PLGA with different LA and GA ratios by mixing DL-lactide and glycolide in the presence of catalyst tin octate $SnOct_2$ in glass ampule under nitrogen atmosphere. The temperature of the reaction was maintained at 160 ºC for 23 hours. The reaction mixture in the ampule was cooled to room temperature and the resulting polymer was dissolved in methylene chloride. After complete dissolution, the mixture was precipitated in excess of methanol in order to remove impurities. The final product was then vacuum dried at 40 ºC for 48 hours. Varying the amounts of LA and GA resulted in yielding polymer compositions of 82/18, 72/28, 60/40 and 45/55. The molecular weights obtained for these different ratios were in the range of 13000-17000 Da.

Ajioka et al.[25] reported the synthesis of high molecular weight PLGA (i.e., 160 kDa) by using a azeotropic solvent like diphenyl ether, they did the azeotropic dehydration of mixture of L-lactic acid and glycolic acid at 130 ºC for 20-40 hours using tin powder as catalyst.

The main challenge in polycondensation reaction for PLGA is the formation of water during the synthesis which results in formation of low molecular weight PLGA. Also, if high temperature and high vacuum are applied to reduce the hydration effect, then in that case the equilibrium of product formation is shifted towards reactants side which also results in obtainment of low molecular weight PLGA.[26]

Ring opening polymerization of lactide and glycolide in the presence of a metal catalyst at high temperature (130-220 ºC) can be employed to

synthesize high molecular weight PLGA. The commonly used metal catalysts are 2-ethylhexanoate, tin (II) alkoxides, aluminium isopropoxide and stannous octoate ($SnOct_2$).

In ring opening polymerization for synthesis of PLGA, the first step is dehydration and melting of lactic acid and glycolic acid and the second step involves the depolymerization of lactic and glycolic acid using a catalyst at high temperature (130-270 ºC) and low pressure (2-8 kPa). Lactide and glycolide formed in the previous step are then reacted at 140 ºC under high vacuum using tin octoate as catalyst. A similar method was adopted by Zhou et al.[27] where they synthesized PLGA following the same procedure as mentioned above and they obtained PLGA with LA/GA of 85/15 and molecular weight of 94000 Da. A schematic of ring opening polymerization of lactide and glycolide to synthesis PLGA is represented hereafter:

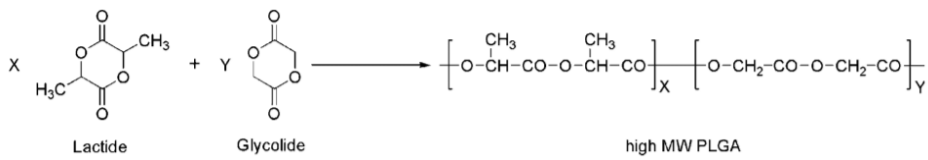

Figure 2: Synthesis of high molecular weight PLGA by ring opening polymerization.[26]

Instead of tin octoate, stannous octoate ($SnOct_2$) can also be used as a catalyst which is highly efficient commercial catalyst and since it is also permitted as a food additive in different countries.[28]

Duval et al.[29] synthesized PLGA by using three different catalysts namely stannous octoate, zin lactate ($ZnLac_2$) and bismuth subsalicylate (BiSS), as these three catalysts have low-toxicity and have applications in medicine. In their synthesis procedure, DL-lactide and glycolide were fed into a 100 ml round bottom flask and heated up to 150 ºC. After the previous step, defined amount of benzyl alcohol and catalysts were added. The catalyst to initiator ratio was kept at 0.03. After catalyst addition, acidic ethanol was also added. For three different catalysts i.e., $SnOct_2$, BiSS and $ZnLac_2$, the polymerization time was 1, 6 and 8 hours at 150 ºC. The reaction medium was dissolved in chloroform and hexafluoro isopropanol mixture and then precipitated in ethanol. The molecular

weight obtained from $SnOct_2$ and BiSS was obtained to be 21500 and 22200 g/mol with LA/GA ratio of 71/29 and 69/31, respectively. In another synthesis, using $SnOct_2$ and BiSS higher molecular weight PLGA was also obtained in the range of 71000-95000 with LA/GA ratios of 44/56, 37/36 and 44/56, 42/58, respectively. Conclusively, $SnOct_2$ had faster polymerization rate than other two catalysts but purification of PLGA is needed for biomedical applications.

In order to obtain high molecular weight PLGA, there are some parameters that must be kept in mind like purity of the monomers. If the moisture content in the lactide and glycolide is high, then it is difficult to obtain PLGA with high molecular weight. It is because the moisture content can terminate the chain growth and also increases the side reactions or shift the equilibrium of the polymerization. That is why high vacuum or inert atmosphere is provided in order to prevent side reactions and other changes in the polymerization reactions.[26] The polymerization time is related to the amount of catalyst used, if high amount of catalyst is used then short polymerization time is required. With increase in polymerization temperature lower amount of catalyst is required if the temperature is increased above 190 ºC then polymer decomposition starts.[30]

In this section, physico-chemical properties, and synthesis of PLGA were discussed in detail. In the following section, synthesis of polymeric NPs (PNPs) via different techniques will be highlighted.

1.3 Synthesis of Polymeric NPs (PNPs)

PNPs are synthesized by various techniques which can be categorized into four groups. First one is emulsion-based synthesis which includes single, double, and multiple emulsions. Second is precipitation-based synthesis including nanoprecipitation, salting out, rapid expansion of supercritical fluid into liquid and dialysis. Third is by direct compositing methods, i.e., melting technique, spray drying, in situ forming micro-particles and supercritical fluid. Fourth involves new techniques like microfluidics and template/mould based technique. In this section, PLGA NPs synthesis methods will be discussed briefly since PLGA NPs have been used for encapsulation of IONPs in this project.

1.3.1 Single Emulsion Method

Single emulsion method, being a simple nanoparticle synthesis method has been used for encapsulation of various hydrophobic drugs by PLGA. In this technique, first the hydrophobic moiety and the polymer are dissolved in a solvent which is water immiscible and then emulsification of this solution is done in the water and stabilizer solution using an ultrasound or a homogenizer.[31] Removal of oil phase from the emulsion can be done either by evaporation under vacuum or by solvent extraction yielding dispersed NPs in water. Impurities like free drug or free polymer are removed from the obtained product by centrifugation and washing with pure water. Solvents that are commonly used for this process are ethyl acetate, dichloromethane, chloroform etc. Drugs like cyclosporin A, docetaxel, DOX and paclitaxel have been encapsulated by PLA, PLGA and their modified forms using single emulsion method.[32-35] High encapsulation efficiencies can be obtained using this process and hydrophobic drugs can successfully be encapsulated by various polymers. The main challenge is the encapsulation of hydrophilic moieties because of the diffusion of moieties from emulsion to aqueous phase.[36] Another challenge in this technique is the interaction of drug and surface of NPs rather than the encapsulation inside the polymer which results in burst release of drug upon administration. An illustration for single emulsion process is shown in figure 3.

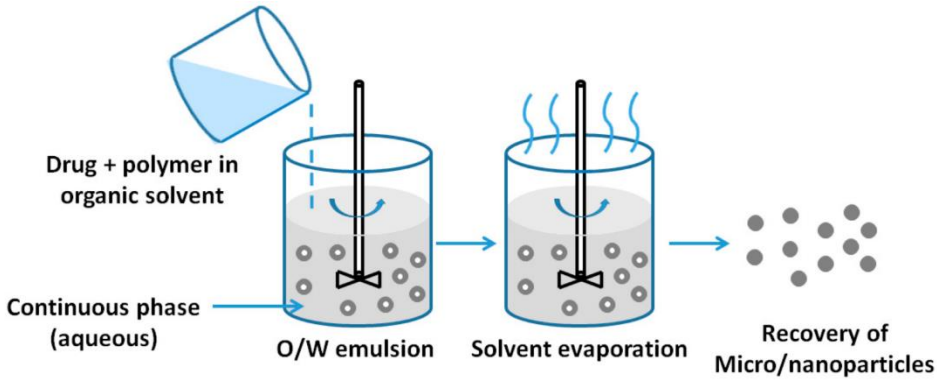

Figure 3: Illustration of single emulsion solvent evaporation process. [37]

1.3.2 Double Emulsion Method

The above-mentioned challenges are overcome by modification of process from single emulsion to double emulsion technique. In double emulsion technique, two aqueous layers exist and are separated by an oil layer. In this technique, emulsification of aqueous drugs is done in organic solvent containing polymer. This emulsion is then again added into an aqueous phase containing the emulsifier forming a double emulsion. The organic solvent is evaporated resulting in formation of nano/microparticles. The organic solvent must have a low boiling point in order to facilitate the evaporation at a lower temperature. The obtained NPs are then centrifuged, washed several times, and redispersed in water. Commonly used solvents are acetonitrile, chloroform, benzene, methylene chloride and ethyl acetate etc. An illustration for the following process is shown in figure 4.

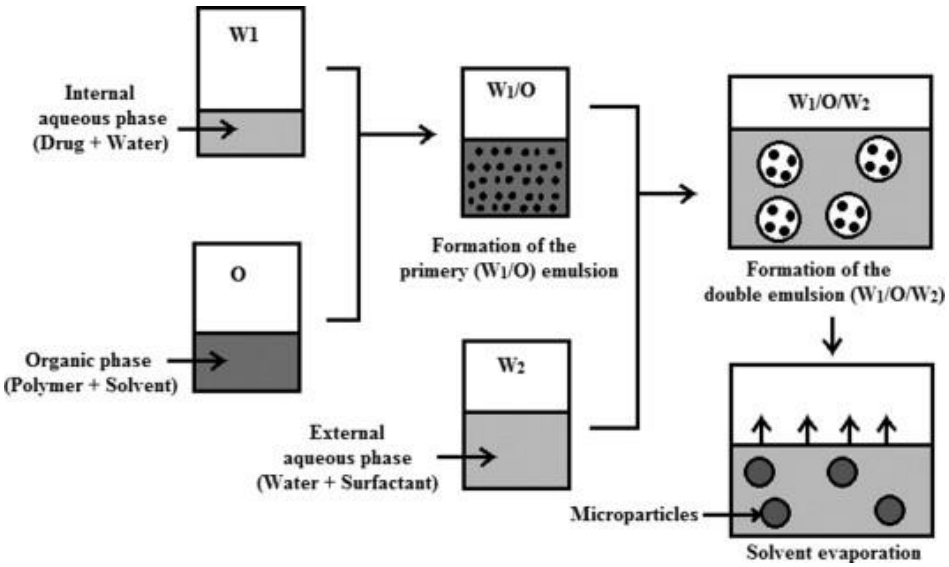

Figure 4: Illustration of double emulsion solvent evaporation process. [38]

Uhicda et al.[39] synthesized PLA and PLGA microparticles loaded with ovalbumin (OVA) using double emulsion solvent evaporation method. Sodium Chloride (NaCl) was added in the aqueous phase as a stabilizer. It was observed that the presence of NaCl had influenced the release of OVA. In absence of NaCl rapid release of OVA was observed whereas the presence of NaCl, facilitated a sustained-release profile. Irregularities in microspheres morphology was also observed in the absence of NaCl. With increase in M.W and particle size a decrease in the release rate was observed. The reason for the former was the flocculation of microparticles and decrease in the surface area of microparticles which had impacted the release of OVA. For the later, interaction of amino acids of OVA and acidic carboxyl groups of PLGA might be the reason of decrease in release rate.

In double emulsion technique, parameters like stirring rate of emulsification, ratio of aqueous to organic phase and type of emulsifier can largely influence the size and morphology of NPs obtained. It also impacts the loading and release efficiency of various drugs.

1.3.3 Salting-out Technique

Salting-out is also a technique which can be employed to obtain NPs by dissolving polymer and drug into a water-miscible solvent like tetrahydrofuran, acetonitrile and adding this solution into salting-out agent containing aqueous phase. Stabilizers such as polyvinylpyrrolidone (PVP) are also used along with salting-out agents. The emulsion obtained is then diluted by excess water facilitating the diffusion of water miscible solvent into aqueous phase and resulting in formation of NPs. NPs are then obtained by centrifugation and washed several times with water before further application. Commonly used salting-out agents are magnesium chloride and calcium chloride. The main advantage of this process is that it can be done at room temperature and it will enhance the drug loading efficiency of heat sensitive drugs. Various parameters have an influence on size and morphology of NPs such as type and amount of salt used and ratio of polymer and solvent.[40] Although this technique is widely used for forming PNPs, but limited literature sources are available for use of this technique for drug loading.

1.3.4 Super-critical Fluid Technology

Another technique which is quite efficient in encapsulation of various drugs into polymer matrices is super-critical fluid technology. In this technique, a supercritical fluid such as carbon dioxide (CO_2) is used to dissolve a polymer and drug. The rapid expansion of this mixture results in formation of NPs. This technique involves two principal processes, one is the rapid expansion of supercritical solution (RESS) while the second is the rapid expansion of supercritical solution into a liquid solvent (RESOLV). The limitation of RESS is that it can only be used for low drug concentration and low molecular weight.[31, 41] Due to the above-mentioned limitations, several modifications have been made in this technique to produce better NPs. A technique named supercritical anti-solvent (SAS) was introduced to synthesize drug loaded PLA and PLGA NPs. In SAS, the drug and polymer solution are precipitated into a supercritical fluid which dissolves the organic solvent resulting in NPs formation. Fatemeh et al. [42] synthesized curcumin loaded PLGA NPs by using a modified SAS technique. They studied the effect of various parameters i.e., addition flowrate of solution into supercritical fluid,

ultrasonic power effect, molar ratio of CO_2 to solvent etc. all these factors contributed to affect the size and loading efficiency of NPs. Although, this technique facilitates the synthesis of NPs with least amount of impurities and residuals, but the operating cost for these processes is quite high. Also, there is a difficulty in dissolving strong polar solvents into CO_2 and cosolvents and surfactants are required which complicates the process.[43]

1.3.5 Spray Drying Technique

Instead of using a supercritical fluid, spray drying technique was first invented by Pamujula et al.[44] in 2004 in order to eliminate the use of supercritical fluid and also reduce the operating cost. This technique provides efficient encapsulation efficiency of hydrophilic drugs such as ceftazidime, ciprofloxacin, and proteins etc. In this technique, a polymer is first dissolved into an organic solvent which is volatile and then mixed with aqueous drug solution forming an emulsion. The emulsion is then sprayed through a standard nozzle into a hot nitrogen chamber resulting in formation of NPs, which are dried and washed afterwards for further use. The drug loading efficiency of hydrophilic drugs is less compared to hydrophobic drugs due to the weak affinity between the hydrophilic drugs and the polymer. So, by modifying the spray drying technique, a hydrophobic drug like doxorubicin was loaded in PLGA NPs by Merkulova et al.[45] where they used a BUCHI spray dryer B-90. In literature, usually microparticles are obtained by this technique, but the above-mentioned author has synthesized NPs using this technique. PLA NPs were loaded with salbutamol-sulfate (hydrophilic drug) and beclomethasone dipropionate (hydrophobic drug) by Hirvonen et al.[46] They obtained NPs around 200 nm and drug entrapment efficiency was above 50%. An important parameter in this method that influences the size is the flow rate at which spray drying occur and the polymer content. Variation in the flow rate results in different sizes of NPs and increase in the flowrate results in larger NPs.

1.3.6 Microfluidics

The use of microfluidics technique has increased during the past decade because of their extensive use in synthesizing NPs. Although in the past it was employed for synthesis of MPs but now after modifying the microfluidic chips and setups, NPs can easily be synthesized and monodisperse populations can be attained. Microfluidic devices have different processes for generation of droplets and hence different applications. Commonly used microchannels are Terrace, T-junction, flow-focusing (FF) and Y-junction. The images of these micro-channels are hereafter:

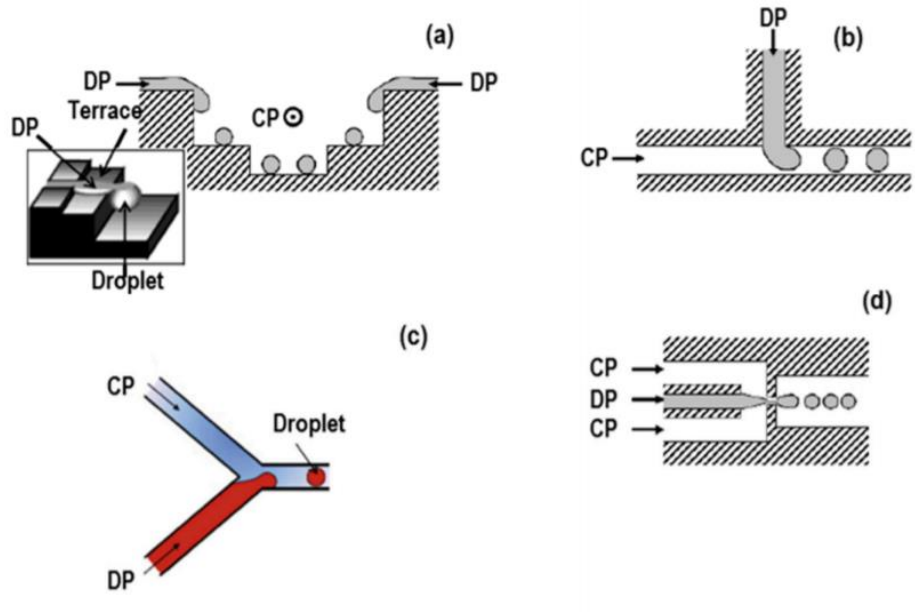

Figure 5: Illustration of different microfluidics channels. (a) terrace, (b) T-junction, (c) Y-junction and (d)flow focussing[47]

All these types of channels can be utilized to synthesize NPs and MPs of various sizes. In literature, modifications in flow focusing microchannels have been made in order to obtain NPs.[48] As seen from image d, in FF, the dispersed phase flows through the centre of the chip while the continuous phase comes through the channel surrounding the centre. Both these phases are mixed at the narrow-restricted point which results in generation of droplets. Minsoung et al. synthesized PLGA-PEG NPs using

a modified version of FF i.e., 3D hydrodynamic flow focusing (3D HFF) microfluidics setup. They argued that while using conventional 2D HFF, polymers with high M.W cannot be used to synthesis NPs since they aggregate or interact with the hydrophobic channels and cause increase in internal pressure resulting in failure or clogging of chip.[49] In this method, PLGA-PEG was dissolved in acetonitrile (ACN) and flowed through microfluidics channel with water as continuous phase, the restricted channel resulted in formation of PLGA-PEG NPs. They varied the M.W of PLGA and also increased the concentration of PLGA-PEG which resulted in obtainment of NPs in range of 50-200 nm. An illustration of the 3D HFF setup and NPs obtained from the process is depicted in figure 6 [49]:

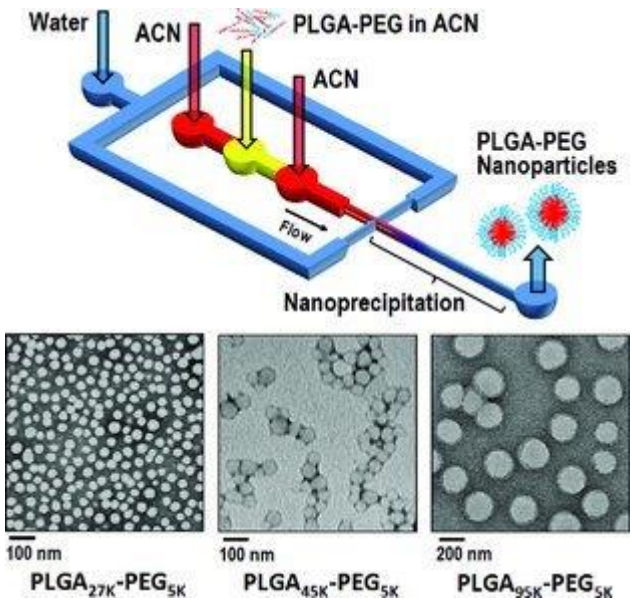

Figure 6: Illustration of 3D hydrodynamic flow focusing setup for synthesis of PLGA-PEG NPs.

The PNP synthesis techniques discussed in Section 1.3 have several advantages and disadvantages. Although, these techniques have been employed for synthesis of NPs, these techniques still lack to provide reproducibility of the results. All these techniques are sensitive to small changes in parameters. For instance, in single or double emulsion method if aqueous/organic ratio or the stirring rate for emulsion formation is

changed. It will greatly influence the size of particles and microparticles will be formed instead of NPs. Similarly, in salting out technique if salt concentration is varied, this will greatly influence the size.

So, in this report, a simple technique was opted for synthesis of PNPs which ensures reproducible results, the technique is nanoprecipitation. This technique has been widely used for synthesis of PNPs with higher reproducibility compared to any other technique. Nanoprecipitation is an easy one step technique which is fast and has low electric power consumption. In other techniques like emulsion-diffusion, emulsion-evaporation and salting out emulsion precursors are necessary while this technique is based on just two phases without any precursor involved. On the other hand, NPs in the size range of 50-500 nm are obtained with a higher reproducibility.[50] Also, drugs and various inorganic NPs are encapsulated into polymer structures using this technique. Nanoprecipitation will be touched upon in detail which will include the illustration of mechanism and various applications for drug release in the next section.

1.4 Nanoprecipitation

Nanoprecipitation also known as solvent displacement technique was developed by Fessi et al.[51] This technique is one of the simplest methods by which organic/inorganic moieties can be encapsulated by a polymer matrix. Nanoprecipitation is used for synthesis of polymeric nanoparticles. This method involves the mixing of two phases namely a solvent phase and a non-solvent phase. The solvent phase consists of an organic solvent in which an organic/inorganic moiety is dissolved while the non-solvent phase mostly contains water and a surfactant that prevents aggregation of NPs and provide stability to the NPs.[52]

In this method, typically a drug or some other moieties are first dissolved into the organic solvent and this solvent phase is then added dropwise into the non-solvent phase containing surfactant and water. The organic solvent used is miscible in water while the dissolved moiety/drug or polymer are insoluble in water causing them to precipitate and form a globule structure. The surfactant in the non-solvent phase provides the stability to these globule structures. There are two mechanisms which explain the formation of NPs in nanoprecipitation. One is the phenomena that govern the dissolution of solvent phase into the non-solvent phase is Gibbs-Marangoni effect which states that the mass transfer between the fluids occurs due to the surface tension gradient. Second is the explanation of NPs formation via Classical Nucleation Theory. Both of the above mentioned mechanisms are discussed in detail in the following section.

1.4.1 Mechanism of Nanoprecipitation

Quintar et al. and Galindo et al.[53, 54] proposed a mechanism for formation of NPs in nanoprecipitation by interfacial turbulence or Gibbs-Marangoni effect. This mechanism is based on differences in surface tension of the solvent (organic solvent + polymer) and the non-solvent (surfactant + water) phase. Non-solvent phase has a high surface tension and has a stronger pull on the surrounding liquid while the surface tension of the solvent phase is low. This difference in surface tension causes turbulence at the interface of solvent and non-solvent phase which leads to eddies formation at the interface of both phases. These eddies result in increased mass transfer from one phase to another. Since the solvent phase

is miscible in non-solvent phase, the solvent phase starts to break down into smaller and smaller droplets resulting in dissolution of solvent into non-solvent phase and precipitation of polymer as NPs. The interfacial tension gradient can be calculated by Marangoni Number (Ma). Instability in the system can only be caused if the value of Ma is greater than the specific values of solvent and non-solvent phases. In cases, where concentration gradient is responsible for surface tension gradient, the Ma is given as:

$$Ma = \Delta\Upsilon.\Delta C/\eta.D_{AB} \quad (1)$$

Where $\Delta\Upsilon$ is interfacial tension gradient, ΔC is concentration gradient, η is viscosity of organic phase and D_{AB} is diffusion coefficient of organic phase in aqueous phase. The schematic of this mechanism is shown as below [55]:

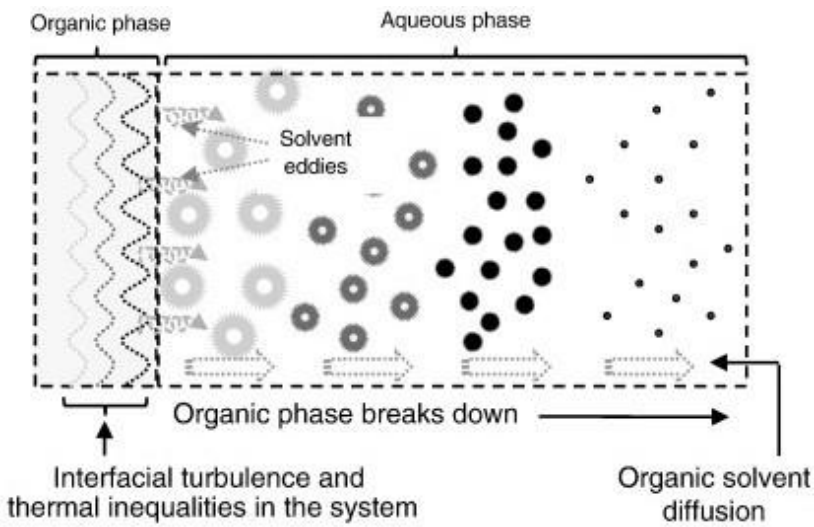

Figure 7: Schematic of mechanism of nanoprecipitation explained via Gibbs-Marangoni effect.

Although, Gibbs-Marangoni effect is the most popular mechanism by Ostrovsky et al.[56] showed that increase in concentration of organic solvent in water results in decrease in ΔϒΥ. Thus, the Marangoni effect decreases and hence the mass transfer from one phase to another will also decrease. In this study, they argued that natural convection and forced mixing influence the intensity of mixing which is dependent on the mixture density.

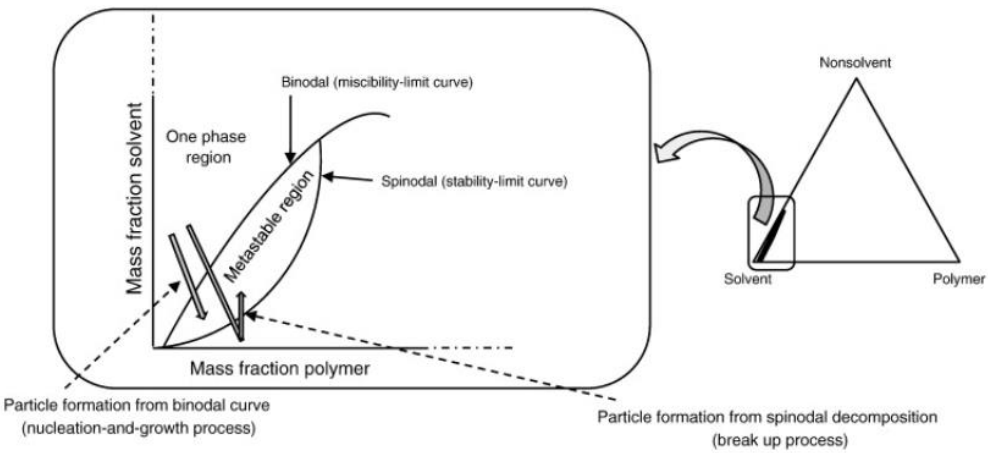

Figure 8: Ternary phase diagram for solvent, non-solvent, and polymer.

Many researchers have tried to explain the mechanism of nanoprecipitation based on Classical Nucleation Theory. Beck et al.[57] did an extensive study in order to verify the concept of Ouzo effect presented by Katz et al.[58] and Aubry et al.[59] in nanoprecipitation with and without usage of surfactant. The occurrence of ouzo effect is due to the rapid transfer of a hydrophobic solute (i.e., polymer) into metastable region (ouzo region) which is in between the binodal (miscibility-limit curve) and spinodal (stability-limit curve) boundaries in a ternary phase diagram. A ternary phase diagram of solvent, non-solvent and polymer is presented as under[55]:

Since the hydrophobic solute is dissolved in a solvent and due to miscibility of solvent into the non-solvent phase. The solvent diffuses into the non-solvent phase and this leads to precipitation of hydrophobic solute

and generation of local supersaturation of hydrophobic solute in the system. This precipitation of hydrophobic solute leads to formation of nuclei of hydrophobic solute. When the nuclei radius becomes larger than the critical nuclei radius, they continue growing until the system reaches equilibrium. The critical nuclei radius is dependent on surface tension between two phases and the difference between free energy per unit volume. The equations for nucleation and critical radius are given as follows:

$$J = \frac{2D}{d^5} \exp\left(-\frac{16\pi \gamma^3 \tilde{v}^2}{3k_B^3 T^3 [\ln(S)]^2}\right) \quad (2)$$

$$r^* = -\frac{2\gamma}{\Delta g_v} \quad (3)$$

Where D is polymer molecular diffusion, d is polymer molecular diameter, T and k_B are absolute temperature and Boltzmann constant, γ is the interfacial tension between already formed NPs and bulk solution, $\tilde{v}$ is molecular volume of polymer and S is the supersaturation defined as the ratio of actual polymer concentration and solubility of polymer in solvent mixture. Δg_v is the difference of free energy per unit volume.

The growth rate of NPs (G) is dependent on the molecular weight (M_w), concentration (c) and density of polymer (ρ), the mass transfer coefficient (k_m), and the supersaturation (S). The equation for this relation is given as below:

$$G = \frac{2k_m M_w c}{\rho}(S-1) \quad (4)$$

Particle aggregation can be caused by Ostwald ripening phenomenon or by encountering of particles with each other due to Brownian motion and fluid motion. All these phenomena govern the final particle size of NPs. The aggregation due to Brownian motion and fluid motion is influenced by dynamic viscosity of dispersive medium, temperature, radii of colliding particles and shear rate (velocity gradient) respectively. The particle size can be estimated as a function of aggregation time given as:

$$d^3 = \frac{8k_B T \rho_{sol} f_s f_p^i}{\pi \rho_p \eta} \times t \quad (5)$$

Where T is temperature, ρ_{sol} and ρ_p are densities of dispersive medium and particles, respectively, f_s is the mass fraction of solvent, f_p^i is the initial mass fraction of polymer in solvent, d is the diameter of NPs and η is dynamic viscosity of dispersive medium. It is evident that the final NP size is governed by aggregation phenomena and role of stabilizing agent during the nucleation and growth process. Thus, in this mechanism, interaction between polymer and the active substances plays a crucial role in determining the size of NPs.

Gibbs-Marangoni and Classical Nucleation Theory mechanisms can be summarised based on the difference in driving forces. In the first mechanism, the driving force is the surface tension gradient which causes fluctuations in mechanical equilibrium of the system resulting in lowering of free energy and generation of NPs. Also, in this mechanism, the factor that governs the particle formation is the physiochemical properties of organic phase and its interaction with the non-solvent phase. In the second mechanism, the driving force is the hydrophobicity of the polymer that leads to generation of supersaturation and polymer precipitation. The three parameters i.e., composition, interaction and physicochemical properties of polymer/solvent/non-system influence the particle formation. Stainmesse et al.[60] hypothesized that, at low organic/aqueous ratio and polymer concentration, nucleation and growth process are responsible for the particle formation while at higher polymer concentration and aqueous ratio Gibbs-Marangoni effect is the dominating mechanism.

The next section will focus on the factors that can affect the NPs size in nanoprecipitation.

1.4.2 Factors affecting particle size in Nanoprecipitation

Several factors can influence the size and morphology of NPs in nanoprecipitation. The factors that have been studied by most of the researchers are concentration of polymer, organic/aqueous phase ratio, addition rate of organic phase, nature of solvent, molecular weight of polymer. All these factors will be discussed in detail with the support from literature.

1.4.2.1 Effect of Polymer Concentration

In most of the research studies, it has been observed that the polymer concentration has largely influenced the size of NPs. In one of the studies, PLGA concentration was changed from 5 to 15 mg/ml and an increase in size from 157 to 194 nm was obtained. This can be explained based on Classical Nucleation Theory where an increase in super-saturation will occur because of the increase in polymer chains in the solvent phase. An increased number of nuclei will be formed, and the growth rate of NPs will also be fast. Hence increasing polymer concentration will increase the growth rate of NPs resulting in attainment of bigger NPs. The second reason is the increase in the viscosity of organic phase caused by increasing concentration of polymer. Since the amount of polymer in the drop will substantially increase, the precipitation of polymer from the solvent will be hampered due to slower diffusion of solvent into the non-solvent phase resulting in larger NPs.[61]

Another study showed a similar effect of concentration on the size of NPs. By increasing the polymer concentration from 5 to 20 mg/ml, an increment in the size was obtained from 202.5 to 246 nm. This increase can also be based on the ratios of lactide (LA) to glycolide (GA) in PLGA. LA group is more hydrophobic compared to GA, hence if the ratio of LA is greater than GA then NPs with smaller size will be obtained and if the drug is encapsulated in such PLGA, a decrease in drug release rate will be observed.[62] The reason for smaller size could be that since, the polymer is more hydrophobic it will try to reduce its interaction with the non-solvent phase as much as possible, so the polymer will shrink more

resulting in smaller NPs. An opposite affect will be observed compared to above explanation if the ratio of GA is more than LA.

1.4.2.2 Effect of Organic/Aqueous Ratio

Madani et al.[63] studied the effect of organic/aqueous phase ratio on size of PLGA NPs and found that by keeping a constant amount of aqueous phase and increasing the amount of organic phase from 1 to 3 ml, a decreasing size was obtained in the range of 478 to 300 nm. This could be because of decrease in viscosity of the organic phase and lowering of polymer concentration resulting in smaller NPs as explained in above paragraph. Larger NPs size was obtained when volume was increased from 3 to 6 ml and it was argued that this might have happened because of Ostwald ripening since the solvent evaporation in this case would take longer time and NPs will have a chance to grow more. A completely different trend for this effect was observed by Budhian et al.[64] where they found that increasing the volume of organic phase did not affect the size of NPs, but the drug content decreased from 1.8 to 1 %. Reducing the solvent volume resulted in increased drug content which could be explained based on solvent evaporation time which is less in this case and this also allows reduced time for drug diffusion.

1.4.2.3 Effect of Rate of Addition of Organic Phase into Aqueous Phase

The addition of organic phase into the aqueous phase significantly influences the size of NPs. Beck et al.[57] studied the effect of addition of acetone (organic solvent) containing PCL into aqueous phase (Pluronics F68 and water), they observed a decreasing trend of NPs size while increasing the addition flowrate from 3.5 to 10.6 ml/min. They elucidated that increasing the addition flowrate increases the velocity of diffusion of acetone from organic to aqueous phase which results in lowering of polymer/acetone droplet concentration in the aqueous phase and thus smaller NPs are obtained.

A similar reason for reduction in NPs size with increasing addition rate was also provided by Lince et al.[65] where they also investigated the formation of PCL NPs. They deduced that the decreasing size of NPs was probably because of better mixing of two phases which lead to higher

nucleation rate and hence smaller NPs in large population. A decreasing size trend was also observed by Badri et al.[66] while increasing the flowrate of organic phase for encapsulation of indomethacin inside PCL. They argued that larger NPs are obtained at lower flowrate because of non-homogeneous mixing of organic and the aqueous phase.[55]

1.4.2.4 Effect of Nature of Solvent

The nature of solvent greatly influences the size of NPs and this can be considered as the most important parameter. In nanoprecipitation, polymer solubility in organic solvent and the miscibility of organic solvent in water is crucial for the determination of NPs size. The solvent which has higher miscibility in water produces smaller NPs. This is because, the solvent diffusion from the organic phase to the water phase is faster due to higher miscibility and the polymer arranges itself into a smaller size.

Huang et al.[67] estimated the diffusion coefficient of acetonitrile, acetone and THF with and without PLGA into water. They found that acetonitrile has the highest diffusion coefficient compared to acetone and THF. Hence, this hypothesis was confirmed by synthesizing PLGA NPs with smaller size in case of acetonitrile i.e., 150 nm and bigger NPs with THF i.e., 300 nm using same amount of organic solvent under similar conditions. They concluded that if the diffusion coefficient of the solvent is high then small NPs with narrow size distribution are obtained. If diffusion coefficient is low than bigger NPs with broad size distributions are obtained. Methanol and ethanol were also tested and since they are highly soluble with high diffusion coefficient, smaller NPs in 50-100 nm range were produced.

Sahana et al.[68] also studied the effect of solvent on PLGA NPs size, they used acetone, chloroform, dichloromethane, and ethyl acetate to synthesize PLGA NPs. It was found that PLGA NPs were only formed while using ethyl acetate and explained that the interfacial tension in case of ethyl acetate was the lowest compared to the other solvents. Small NPs were obtained while using ethyl acetate as solvent for PLGA but for other solvents, ethyl acetate was mixed in order to get PLGA NPs in the range of 150-250 nm. They argued that interfacial tension and viscosity of the solvent are key factors in determining the NPs size. This argument supports the condition of interfacial tension gradient in Gibbs-Marangoni effect i.e., if the interfacial gradient is high between the solvent and the

non-solvent phase then the Marangoni number will be higher and smaller droplets will be formed at the interface resulting in smaller NPs.

1.4.2.5 Effect of Polymer Molecular Weight

Molecular weight (M.W) of the polymer also has an impact on the size of the NPs. Although, in most cases, a general trend with respect to M.W has not been observed. Most of the researchers have reported various trends based on their systems. Öztürk et al.[69] synthesized PLGA NPs as well as chitosan coated PLGA NPs and loaded them with clarithromycin. PLGA with three different molecular weights i.e., 7000-17000, 24000-38000 and 38000-5400 Da were used to synthesize bare PLGA NPs. They found that the particle size decreased from 154 to 142 nm when the highest molecular weight PLGA was used. The reason could be the increase in hydrophobicity of the polymer due to increasing number of aliphatic chains with increased molecular weight. A similar trend of decreasing NPs size with increasing molecular weight was also observed by Banderas et al.[70] where by increasing the M.W from 12000 to 48000 Da resulted in decrease in particle size from 311 to 89 nm. A similar reason as mentioned above was also provided by the author.

Table 1: Summary of effect of different parameters on size of NPs

Parameters	Effect on NPs size
Polymer concentration	Increase
Organic/Aqueous ratio	Decrease or no change
Rate of addition of organic phase into aqueous phase	Decrease
Nature of solvent	Based on Diffusion Coefficient
Molecular Weight	Decrease

The following section will highlight the applications of PLGA and hybrid PLGA-IONPs in biomedicine. Owing to its biodegradability and biocompatibility, PLGA has vast applications in drug delivery and some of them are discussed in the next section.

1.5 Biomedical Applications of PLGA and PLGA-MAG NPs

In previous sections it has been briefly discussed that PLGA has potential biomedical applications. In this section biomedical applications of PLGA and PLGA-MAG NPs will be discussed in detail. PLGA NPs containing drug can be encapsulated by various techniques that are described in section 1.3. In this section, drug loaded PLGA NPs synthesized by nanoprecipitation will be discussed. The reason is because this report focuses on the polymeric and hybrid NPs synthesized by nanoprecipitation. For PLGA-MAG NPs, different biomedical applications will be discussed in detail.

PLGA has been used as a biomaterial since 1970s as sutures in surgery. The commonly used sutures are Vicryl ® (Ethicon Inc, USA), Dolphin Sutures ® (Futura Surgicare Pvt Ltd, India) and Polysorb ® (Syneture, USA) etc.[21] In the past decade, PLGA has more applications in drug delivery. PLGA has been used as a drug delivery carrier because of its biocompatibility and biodegradability. Some of the PLGA particles products are approved for clinical use as drug carriers such as Lupron Depot ® (Abbot Laboratories, USA) and Trelstar ® (Watson Pharmaceuticals, USA). [21]

Cheow et al.[71] encapsulated a hydrophilic antibiotic into PLGA NPs by using the technique of nanoprecipitation. The antibiotic that is used in this research article is levofloxacin which is a therapeutic drug against pulmonary biofilm infections caused by bacteria and fungus.[72] In levofloxacin loaded PLGA NPs, they used acetone to dissolve PLGA and the drug and the surfactant used was Pluronic-F68. Drug loaded PLGA NPs of 80 ± 30 nm size were obtained in this process and the encapsulation efficiency was obtained to be 16 % which is probably because of the diffusion of the hydrophilic drug in the aqueous phase along with acetone. However, a successful drug loading was obtained in this process.

Different hydrophobic/hydrophilic drugs and inorganic NPs have been encapsulated by various polymers using nanoprecipitation. Chourasiya et al.[73] studied the encapsulation of a hydrophilic drug i.e., atenolol by

PLGA using nanoprecipitation. This drug is extensively used for the treatment of cardiovascular disorders. Chourasiya et al. also studied the influence of various parameters like amount of PLGA, concentration of surfactant and aqueous phase volume on the size and drug entrapment efficiency by a 3^3 factorial design of experiments. The maximum drug entrapment and size obtained were 75 % and 276 nm, respectively. It was concluded that with increase in PLGA amount, the drug entrapment efficiency was seen to be increasing while decreasing the PVA (surfactant) and aqueous phase volume resulted in increase in drug entrapment efficiency.

Fonseca et al.[74] encapsulated paclitaxel (hydrophobic drug) by PLGA. This drug is commonly used for the treatment of various tumors, including lung cancer, breast cancer acute leukaemia etc. Acetone was used as a solvent to dissolve the drug and polymer and this solvent was precipitated into an aqueous poloxamer 188 (non-solvent phase) to obtain NPs. Fonseca et al. used PLGA with different molecular weights and different ratios of LA/GA. It was evident from there results that the incorporation efficiency of paclitaxel was greater than 90% and was independent of molecular weight and their compositions. But an effect on size of NPs was observed, with increase in molecular weight and composition an increase in size was observed from 117 to 160 nm.

Govender et al.[75] studied the encapsulation of a hydrophilic drug i.e., procaine hydrochloride commonly used as anaesthesia by PLGA. They found that the drug entrapment increased by varying the pH from 5.8 to 9.3 from 11 to 62 %. They also tried PLA, fatty acids, lauric acid and other polymers encapsulation along with the drug into PLGA, in order to check the effect of these moieties on the drug entrapment efficiency.

IONPs-PLGA hybrid NPs have also been synthesized for various biomedical applications. The IONPs because of their magnetic properties can be influenced by external magnetic field and hence they help in a targeted action of drug loaded NPs on cancer active sites. Tansik et al.[76] presented a study where they encapsulated IONPs and anti-cancer drug, doxorubicin into PLGA NPs using single oil in water emulsion method (O/W). The IONPs were coated with oleic acid in order to make them hydrophobic so that the encapsulation in PLGA becomes easy. The drug encapsulation efficiency was obtained to be 32 % and 65 % of total drug

was released in 35 days of incubation. An effect of DOX-PLGA-MNPs was also observed on MCF-7 cells (breast cancer cells) and it was found that with increased amount of drug loaded NPs the cell death was approximately 80 %.

Schleich et al.[77] loaded paclitaxel, an anti-cancer drug, into PLGA NPs containing IONPs by emulsion-diffusion-evaporation method. The hydrodynamic size of drug loaded IONPs-PLGA NPs was obtained to be 243 nm and the drug encapsulation efficiency was obtained to be 25 %. The cytotoxicity of drug loaded IONPs-PLGA NPs was done on CT26 colon carcinoma cells and it was found that the drug was able to kill the cells when its concentration was increased from 2-20 µg/ml. In this study they also preformed anti-tumor efficacy test of multifunctional NPs on CT26-tumor bearing mice and found that these NPs delayed the tumor growth better than the other treatments.

In this introduction section, an overview of IONPs and polymer like PLGA including their physico-chemical properties and synthesis procedure was presented. Different techniques to synthesis PNPs were also highlighted. Nanoprecipitation along with its mechanisms and factors that affect the NPs size was discussed in detail. In the end of this section biomedical applications of PLGA and PLGA-MAG NPs were set forth. In the upcoming section, materials and methods used in this report are discussed in detail.

2. Materials and Methods

2.1 Materials

Iron (III) chloride hexahydrate ($FeCl_3.6H_2O$), iron (II) chloride tetrahydrate ($FeCl_2.4H_2O$) and ammonia solution were purchased from Sigma Aldrich, Germany for the synthesis of magnetite. Milli Q-water was used for the synthesis of magnetite. Poly (lactide-co-glycolide) acid with molecular weight 7000-17000, poly (lactide-co-glycolide) acid with molecular weight 24000-38000, poly (lactide-co-glycolide acid with molecular weight 30000-60000, pluronics F127 and dimethyl sulfoxide (DMSO) were also supplied by Sigma Aldrich, Germany

Note: The three PLGAs with different molecular weight are named as PLGA-1(Mw: 7000-17000) (LA 50: GA 50), PLGA-2 (LA 50: GA 50) with Mw: 24000-38000 and PLGA-3 (LA 50: GA 50) with Mw: 30000-60000 respectively.

2.2 Synthesis Methods

In this section, the procedures that we followed to synthesize IONPs by co-precipitation method and PLGA NPs synthesized by nanoprecipitation are highlighted. The procedure for PLGA-MAG NPs synthesized using the technique of nanoprecipitation is also discussed in detail in this section.

2.2.1 Synthesis of IONPs by co-precipitation

For the synthesis of IONPs by co-precipitation, 84.6 mg of MQ water was weighed in a beaker and 15.4 ml of 25% (vol%) ammonia solution was added into it. 4 grams of $FeCl_2.4H_2O$ and 10.8 grams of $FeCl_3.6H_2$ O were weighed carefully and dissolved in MQ water in a 50 ml volumetric flask. The mixture was shaken well until no undissolved traces were left in the solution. 10 ml from the prepared solution of iron precursors was then added dropwise using a burette into 100 ml of 1M aqueous ammonia solution under constant agitation. It was observed that the iron oxide NPs readily started to form as the iron mixture was added into the ammonia solution. The obtained NPs were then magnetically separated and washed three times with MQ water. Finally, IONPs were dispersed in 12 ml MQ water. These IONPs were then characterized using DLS and HR-TEM.

The image of the setup for IONPs synthesis and the magnetic separation step is shown below:

(a) 

(b) 

Figure 9: (a) setup of synthesis of IONPs and (b) magnetic separation of IONPs during washing step.

2.2.2 Synthesis of PNPs by Nanoprecipitation

For the synthesis of polymeric NPs, nanoprecipitation technique was used. Firstly, 20 mg of poly (lactide-co-glycolide acid) (with molecular weights 7000-17000, 24000-38000 and 30000-60000) were weighed in different vials and 1 ml DMSO was added in each vial. All the PLGA's were dissolved in DMSO under constant stirring. Secondly, a stock solution of 5mg/ml aqueous pluronics F127 was prepared. In three different vials, 20 ml of solution was poured from the stock solution in each vial. The 1ml polymeric solution for each PLGA was injected dropwise into the aqueous pluronics F127 solutions using a syringe pump at a flowrate of 4.5 ml/hr. These three polymeric mixtures were then kept on constant agitation for 5 hours. After 5 hours, the solutions were transferred into eppendorf tubes

and centrifuged at 14500 rpm for 20 minutes. PNPs were obtained at the bottom of the eppendorf tube and the supernatant was thrown away. The PNPs at the bottom were redispersed into known amount of MQ water and characterized using DLS. The image of the nanoprecipitation setup is shown in the following figure:

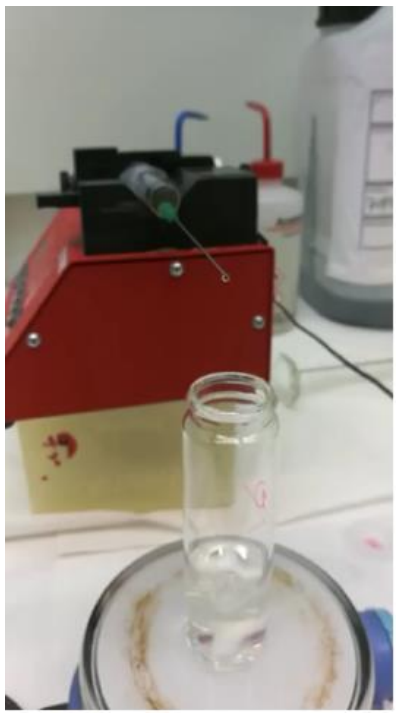

Figure 10: Nanoprecipitation Setup

2.2.3 Synthesis of PLGA-MAG NPs by Nanoprecipitation

IONPs synthesized by Co-precipitation method were encapsulated by three different molecular weight PLGA's using Nanoprecipitation. In this method, the required amount of IONPs (synthesized as mentioned in Section 2.2.1) was taken from the stock solution and was magnetically separated in an eppendorf tube. 1 ml polymeric solution (polymers dissolved in DMSO) was added, and IONPs were dissolved into the solution by vertexing the eppendorf tube for 20 seconds in 3 steps. The

mixture containing IONPs and polymer was then added dropwise into pluronics F127/ water solution using syringe pump at 4.5 ml/hr flowrate. This mixture was then agitated for 5 hours. The encapsulated IONPs were then separated from the eluent by using a magnet. These PLGA-MAG NPs were then washed 3 times with MQ water and redispersed in known amount of MQ water. In this case various magnetic separation times were used which will be discussed briefly into the results and discussion section.

2.2.4 Magnetic Separation Optimization Method

PLGA coated IONPs were synthesized using different concentrations of IONPs i.e., 0.5, 1, 2, 3 and 4 mg. Since IONPs are used in these procedures so the final PLGA-MAG NPs were retrieved using a magnet at different time points. In this section, the magnetic separation time optimization will be discussed briefly. Different studies were performed in order to optimize the magnetic separation time. In first method (M1), PLGA coated IONPs with different concentrations were synthesized and separated on the magnet at 3 different times i.e., 2, 3 and 5 mins. In second method (M1-1), a batch synthesized at a specific concentration of IONPs coated with PLGA was divided into 3 and kept for magnetic separation of 2, 3 and 5 mins. In third method (M1-2), the similar batches as mentioned above were synthesized and kept on the magnet for 45 seconds and then they were divided into 3 for magnetic separation of 2, 3 and 5 mins.

2.2.5 Statistical Design of Experiment for PLGA-MAG NPs

For this study, PLGA-MAG NPs were synthesized same as mentioned in section 2.2.5. But the magnetic separation method adopted by different. For magnetic separation first the whole sample was kept on magnet for 45 seconds and then 7 ml sample was taken into vial for further three time

magnetic separation for 2 minutes in each step. The cleaned sample were then kept for further characterization.

Two statistical design of experiments for the study of affect of different parameters on the size of PLGA-MAG NPs were made in JMP software. In JMP software various statistical analysis methods are present which are helpful for analysis of your data sets. The first design of experiment was a two-level screening design, and the second design was three-level screening design. In screening design, the backward selection of the least significant variable is done by eliminating the most significant variables from the data set. The variable that has the least significant value has the highest effect on the data set.

2.2.6 Coumarin loading in PLGA NPs

For loading of coumarin in PLGA NPs, coumarin was dissolved in DMSO at a concentration of 0.5, 1.0 and 1.5 mg/ml and a stock solution was made for each concentration. From the stock for each coumarin concentration, 1 ml was added into 20 mg of PLGA-1 in a vial and kept for mixing. After proper agitation. The 1ml solution was then filled into a syringe and added dropwise into the non-solvent phase containing 100 mg of dissolved pluronics F-127 in 20 ml of water. The injection rate was maintained at 4.5 ml/hr and the mixture was agitated using magnetic stirrers for 5 hours. After 5 hours, the mixture was then centrifuged for 90 minutes at 12000 rpm. After centrifugation, 15 ml of supernatant was stored to UV-Vis analysis and the remaining 6 ml of sample was again centrifuged for 20 minutes at 14500 rpm. PLGA NPs were seen to be settled at the bottom. The supernatant was carefully removed and added into the stored supernatant. The PLGA NPs were then redispersed in 1.5 ml of MQ water and kept for further characterization.

2.2.7 Coumarin loading in PLGA encapsulated IONPs

From coumarin/DMSO stock for each concentration i.e., 0.5,1.0 and 1.5 mg/ml, 1 ml of sample was taken and added into 20 mg of PLGA-1 in vials. All three vials were kept for mixing and sidewise, the IONPs with amounts 0.5, 2.0 and 4.0 mg were separated on a magnet. The supernatant of IONPs was discard and 1 ml DMSO/Coumarin/PLGA mixture of different coumarin concentrations was added into each IONPs amount in eppendorf. The IONPs were dissolved in the mixture following the similar process as mentioned in section 2.2.4. All three different samples were then filled into a syringe and added dropwise into the non-solvent phase containing 5 mg/ml aqueous pluronics F-127 in 20 ml each. The mixture was then kept for stirring for 5 hours and then the whole stock was magnetically separated for 43 seconds and the supernatant was magnetically separated for 2 mins and kept for UV-Vis. The bottom product was then washed three times for 2 mins using a magnet. The washed sample was then kept for further characterization.

3. Characterization Techniques

In this section all the characterization techniques like used in this report will be discussed briefly including their working principles and characterization methods for our sample analysis.

3.1 High Resolution Transmission Electron Microscope (HRTEM)

HRTEM is a high resolution microscopy tool used for imaging of nanometre scale objects. This instrument shows two dimensional projection of particles and crystals including defects. The working principle of HR TEM is similar to TEM. The instrument uses both scattered and transmitted beam to form an interference image. The interference of electron waves with itself occurs at very low angles during propagation through the objective lens. All the electrons are collected at a particular point on the image plane after emerging from the specimen.[78]

High resolution images were taken using the JEOL 2100 transmission electron microscope (Tokyo, Japan) operating at 200 kV. TEM grids were prepared by placing several drops of the dilute solution on a Formvar carbon-coated copper grid (Electron Microscopy Sciences) and wiping immediately with Kimberly-Clark wipes to prevent further aggregation owing to evaporation at room temperature.

3.2 Dynamic Light Scattering (DLS)

Zetasizer Nano measures the size of the of the NPs based on a technique called DLS. In this process, the Brownian motion of NPs is measured which is related to the size of NPs. In principle, a laser is used to illuminate the NPs and then fluctuation of intensity of light is analyzed. The particles when suspended in a liquid are always in a constant movement due to Brownian motion. This motion is due to random collision of NPs with the surrounding liquid molecules. The motion of larger particles is slower than the smaller particles. Stokes-Einstein equation is used to define the relationship between size of NPs and speed of NPs due to Brownian motion. Since the NPs are in constant motion, the speckle pattern of NPs will also be moving, and the intensity of light will fluctuate because of

motion of NPs. These fluctuations of intensity will then be used to calculate the size of NPs.[79]

To measure the intensity fluctuations, a component called digital correlator is present in the instrument, which measures the similarity of two signals over time. Two signals can be identical if the measurement of intensity signal is done at a very short time after the first measurement. Otherwise, if the comparison of intensity signal is made at a longer time interval, they would not be identical. This correlation is perfect at value 1 and there is no correlation at value 0. Measurement of correlation at various time interval will result in decay of correlation to 0. These correlations are dependent on the size of NPs. If NPs are large, there motion will be slow and hence intensity of pattern will fluctuate slowly and if NPs are small, then fluctuations will be quicker. The correlation function for small and large NPs is shown below:

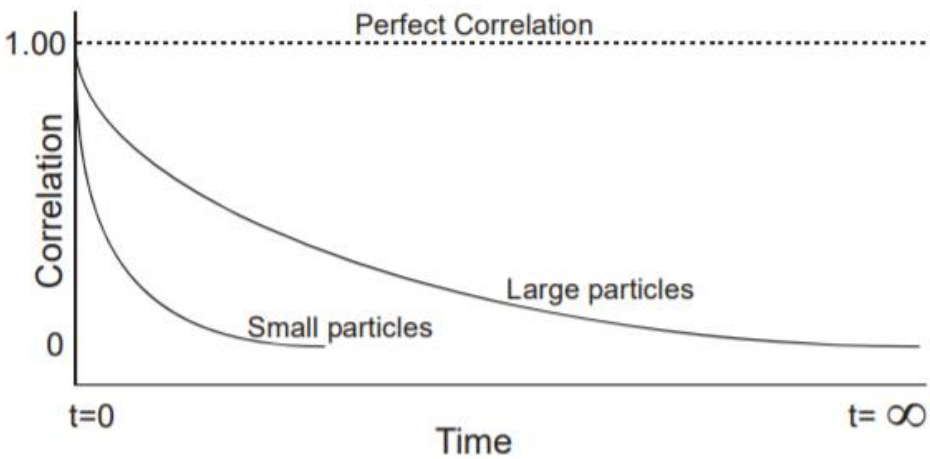

Figure 11: Correlation function for small and large NPs in DLS. [79]

The decay rate of correlation factor for smaller NPs is faster than large NPs. Algorithm is used to obtain a size distribution from this decay rate based on different classes present. A size distribution graphs is given below:

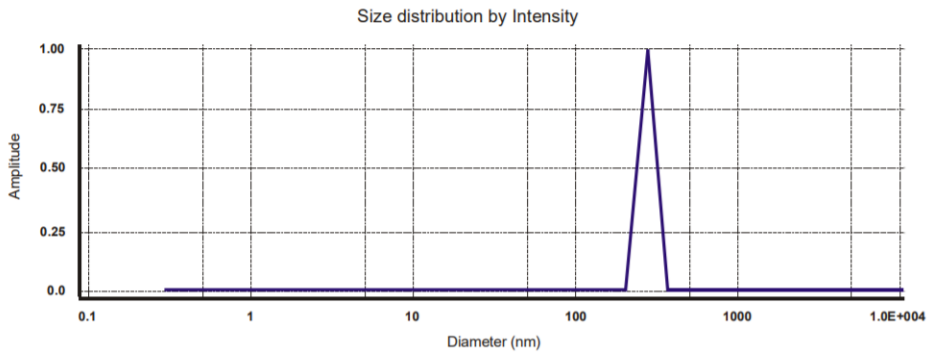

Figure 12: Size distribution graph in DLS. [79]

The DLS usually consists of six main components i.e. (1) a laser, (2) a cell, (3) a detector, (4) an attenuator, (5) a correlator, and (6) a computer. An illustrated image of the process is shown below:

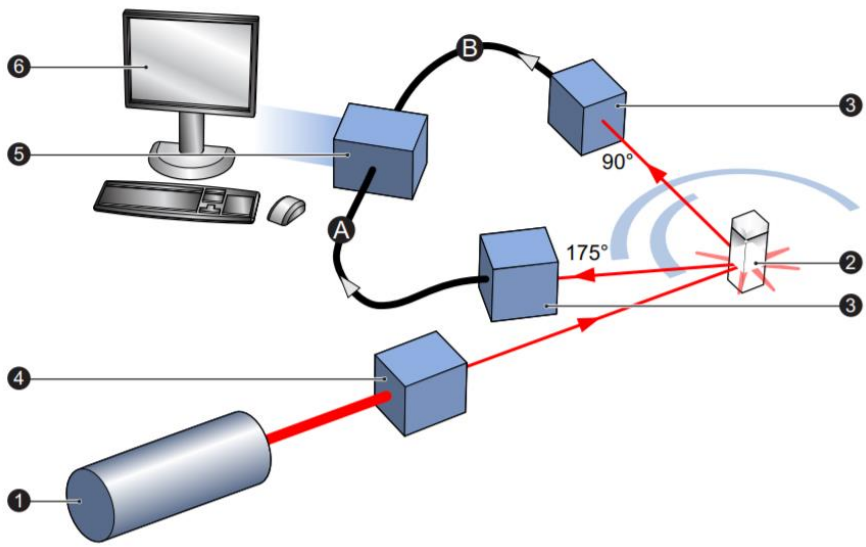

Figure 13: Main components of DLS for size measurement. [79]

A laser is used as a light source which interacts with the NPs inside the cell. Portion of laser beam passes through the sample and rest of it is scattered because of NPs. A detector then analyses the intensity of the scattered light. Since the light is scattered in all the directions by the particles, the intensity of light can be detected from any direction but if

the intensity of light is too much then the detector will be overloaded. An attenuator is used to overcome this challenge, which reduces the intensity of scattered light. A correlator, which is a digital signal processing board, obtains the intensity signal from the detector. The correlator derives the rate of variation in the intensity of signal and pass on this information to a computer where Zetasizer software analyses the data.[79]

3.3 Zeta Potential (ZP) Measurements

ZP of NPs can also be measured using Zetasizer Nano. It is determined by measuring the electrophoretic mobility of the NPs and then by applying Henry equations. Electrophoresis experiment is performed on the sample to obtain electrophoretic mobility and velocity of particles is measured by Laser Doppler Velocimetry (LDV).

The NPs are surrounded by a liquid layer which has two parts; one is a Stern layer where ions are strongly bonded while the other is diffuse layer where the ions are less strongly attached. These two layers exist as an electrical double layer around the NPs. A slipping plane exists within the diffuse layer where motions of ions with the NPs is just inside this boundary. The potential existing at this boundary is the zeta potential. An illustration[79] of the above explanation is as under:

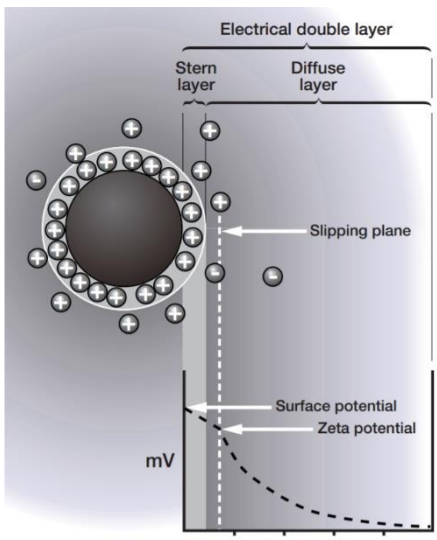

Figure 14: Illustration for electrical double layer, slipping plane, surface and zeta potential points indication.

In electrophoresis experiment, an electric field is applied to the sample where charged particles tend to move towards an oppositely charged electrode due to attraction. This movement is opposed by the viscous forces of particles and when an equilibrium is established between these opposing forces then particles move with constant velocity. This velocity of particles is commonly referred as electrophoretic mobility. Henry equation is then applied to obtain the zeta potential of particles. The equation is given as:

$$U_E = \frac{2\varepsilon\, z\, f(\kappa a)}{3\eta} \qquad (6)$$

Where:

z: ZP

ε: Dielectric constant

η: Viscosity

$f(\kappa a)$: Henry's function

U_E: Electrophoretic mobility

The zeta potential measurement system has seven components, (1) light source, (2) Cell, (3) Detector, (4) Digital Signal Processor, (5) Computer, (6) Attenuator and (7) Compensation Optics. The image of these components is as under:

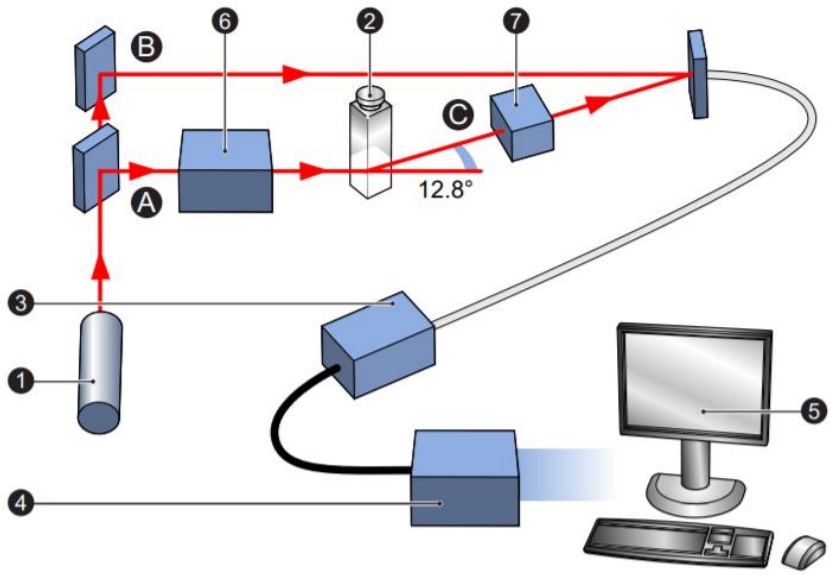

Figure 15: Components of DLS for zeta potential measurements.[79]

In this system, the light source which is a laser is directed at the cell containing the particles, the light source is split into an (A) incident and (B) reference beam, where reference beam provides a necessary Doppler effect. An electric field is applied to the cell which results in motion of particles and hence change in intensity of scattered light which is detected at 12.8 º angle by the detector. This information is then delivered to digital signal processor which is then passed on to the computer where Zetasizer software calculates the electrophoretic mobility and zeta potential of particles. The role of attenuator is to reduce the intensity of scattering and avoid overloading of detector. A compensation optics is also installed to correct the alignment of the scattering beams.[79]

The hydrodynamic and zeta potential of the NPs were measured by using a Malvern Zetasizer Nano-ZS instrument and the data was acquired in

manufacturer's own software. All measurements were performed using aqueous solutions, and results were averaged over triplicate measurements. For magnetic polymeric NPs, the samples were sonicated, pipette flushed and vortexed for three times for 90 seconds before the DLS measurements.

3.4 UV-Vis Spectroscopy

UV-Vis spectroscopy is a common technique used for measuring the absorbance spectra of different compounds in a solution. The electrons of the compound are excited from the ground state to the first singlet excited state because of absorbance of light energy or electromagnetic radiations. The measurements obtained from UV-Vis are based on the principle of Beer-Lamberts law which states that the absorbance of a material is directly proportional to the concentration of species and the length of the path. The equation is represented as:

$$A = -log_{10}\left(\frac{I}{I_o}\right) = \varepsilon C l \qquad (7)$$

Where I and I_o are intensities of incident and transmitted lights, respectively. ε is the extinction coefficient, C is the concentration of species, l is the path length and A is the absorbance.

The UV-Vis spectra for coumarin at different concentrations were obtained by using Cary 60 equipment from Agilent technologies. For drug calibration curve 1 ml coumarin with known concentration was added in cuvette of Cary 60. The UV-Vis spectra were run for wavelength between 600 to 200 nm. For drug loading efficiency measurement, 100 µl from the supernatant of NPs was added into 900 µl of water to obtain a distinct peak in UV-Vis.

4. Results and Discussion

In this section all the results obtained from different studies are discussed in detail with reference to present literature on similar studies. The first section (4.1) starts with the synthesis of IONPs and PLGA NPs using the co-precipitation method and nanoprecipitation, respectively. In the following section (4.2), preliminary studies for optimizing the process of encapsulation of IONPs with PLGA NPs were performed. Two JMP statistical design of experiments for knowing the effect of different parameters on the size of PLGA encapsulated IONPs are presented in section 4.3. In section 4.4, coumarin loaded PLGA NPs and PLGA encapsulated NPs are discussed in detail and the drug loading efficiencies are also presented in that section.

4.1 Synthesis of IONPs and PLGA NPs

4.1.1 IONPs by Co-precipitation

IONPs were synthesized by co-precipitation method (as mentioned in section 2.2.1). These IONPs were characterized using HR-TEM and Zeta Sizer. The HR-TEM* characterization was done by the Co-Supervisor Anuvansh Sharma. The HR-TEM image of IONPs is presented in figure 16. The hydrodynamic size and zeta potential of IONPs was obtained by zeta sizer i.e., 157 ± 11 nm and -36 ± 3 nm, respectively. The average IONPs size was also estimated by counting 100 particles using the software ImageJ and the NPs average size was estimated to be 15 ± 2 nm. The size distribution graph of IONPs obtained from HR-TEM image is also represented in figure 16. The difference in hydrodynamic size obtained from zeta sizer and HR-TEM images is almost ten times and this could be because of the two main reasons. The first reason is that the zeta sizer estimates the hydrodynamic size based on hypothetical sphere which is then calculated using Stoke-Einstein equation[80]. while in HR-TEM gives dry particle size. The second reason could be the aggregation of IONPs due to their close interactions inside the zeta sizer cell during the hydrodynamic size measurements. Cheraghipour et al. also stated that IONPs aggregation occurs because of their hydrophilic nature and sufficient repulsive interactions are required to prevent aggregation.[81]

*HR-TEM characterization by Co-Supervisor: Anuvansh Sharma

As evident from the figure 16, IONPs synthesized by co-precipitation seems to be aggregated, this could probably be because of the three main reasons. The first reason is that there are magnetic dipolar interactions among the formed NPs, and this may lead to aggregation.[82] The second reason could be the lowering of high surface energy, since IONPs have high surface to volume ratio, they have high surface energy and in order to reduce that the IONPs will aggregate. The third possible reason could be the uncoated surface of IONPs, since the IONPs does not have capping agents on the surface. They could easily interact due to inter-molecular forces. Hence the surface needs to be electrostatically or sterically stabilized using different functionalizing agents.

The IONPs have a negative zeta potential because of the presence of hydroxyl groups on the surface of IONPs. These hydroxyl groups make IONPs hydrophilic and they are dispersed well in water. The value obtained for zeta potential is high which means that the IONPs are colloidally stable.[83]

The concentration of the IONPs batch was also estimated by weighing 100 µl of IONPs solution in eppendorf tubes after drying them overnight in an oven. The average concentration of IONPs batch was calculated to be 57±3 mg/ml.

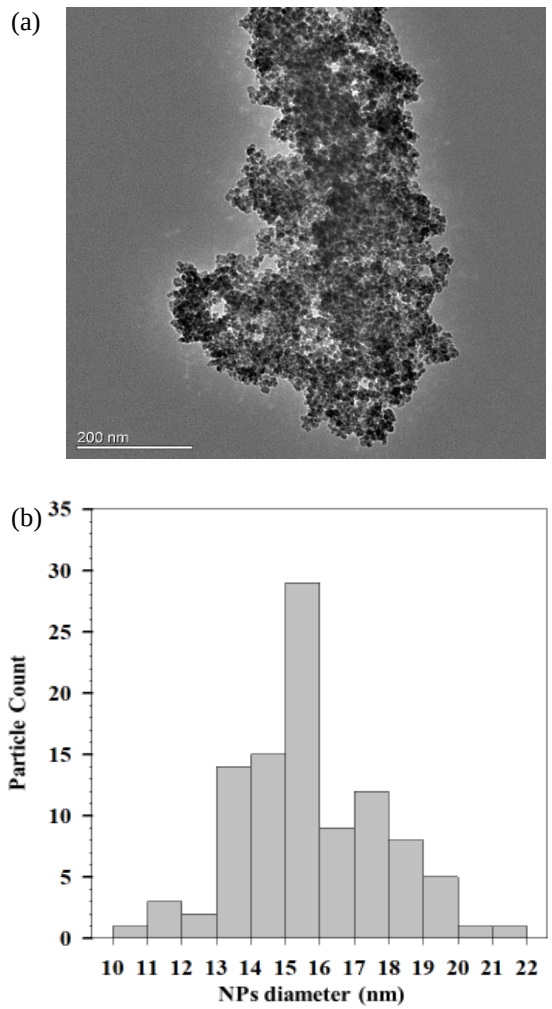

Figure 16: (a) HR-TEM image of IONPs synthesized by co-precipitation and (b) particle count and NPs diameter for 100 particles.

4.1.2 PLGA NPs by Nanoprecipitation

In the previous section, results obtained after characterization of IONPs were discussed in detail. Here in this section, bare PLGA NPs were produced using the technique of nanoprecipitation (as mentioned in section 2.2.2). In this study, NPs with three different molecular weights of PLGA were synthesized by nanoprecipitation as mentioned in section 2.2.3. A whitish layer of PLGA NPs settled at the bottom after the centrifugation is shown in figure 17 (a).

The average hydrodynamic sizes for different PLGA NPs are represented in the figure 17 (a). It was observed that the polymeric NPs size slightly decreased from 109 ± 4 to 84 ± 8 nm with increase in the molecular weight from 7000-17000 to 30000-60000 kDa. The standard deviation for the hydrodynamic sizes is estimated from the average size obtained after repeating the experiments three times. The zeta potential of the PLGA NPs is also plotted and for lower molecular weight PLGA it was obtained to be the highest zeta potential i.e., -32 ± 1 mV and lowest for PLGA-2 i.e., -25 ± 1 mV. A negative zeta potential is obtained for PLGA because of the presence of terminal carboxyl groups (-COOH)[84] on the surface of NPs.[85]

Öztürk et al.[86] synthesized PLGA NPs using PLGA of three different molecular weights i.e., 7000-17000, 24000-38000 and 38000-54000 Da. They used Pluronics F-68 as surfactant and acetone as solvent. The NPs size they obtained was 154 ± 5, 143 ± 1 and 142 ± 3 nm for above-mentioned molecular weights, respectively. Compared to our results, a similar slight decrease in NPs size was observed in this study. The study explained that the decrease in hydrodynamic size with increase in molecular weight could be because of the increased number of hydrophobic chains of PLGA. If the hydrophobicity of the polymer increases, then it will result in smaller NPs size. In their study, the NPs is a bit larger than what we have observed. This could be because of the three following reasons.

- One is the amount of PLGA used in their study is 30 mg/ml while we have used 20 mg/ml.

- Second reason is the use of solvent, we have used DMSO while in their study acetone has been used. Use of different solvents can also greatly influence the NPs size because of their different solubilities in aqueous phase. This has been discussed briefly in section 1.4.2.
- Third could be the use of Pluronics F-127 in our study and Pluronics F-68 in their study. Although, surfactant has important role in stability of NPs, but it can also influence the NPs size.

In our study, for all the PLGAs LA/GA ratio was considered to be 50/50 (as mentioned by manufacturer). Although from the specification sheet it was found that the LA/GA ratio was in the range of 48-52 for all three PLGAs.

The surfactant i.e., Pluronics F127 plays vital role in decreasing the surface tension gradient between the interface of non-solvent phase and solvent phase and prevent NPs aggregation.[87] In literature, pluronics F127 has commonly been used as surfactant because of its low toxicity and good stabilizing ability compared to other surfactants like polyvinyl alcohol (PVA).[88]

Our results from this study show that bare PLGA NPs with high colloidal stability can be synthesized using the method used in this project. Their physico-chemical properties align with similar previous studies, although minor differences can be observed owing to the reasons explained above. In the next section, preliminary studies conducted for the encapsulation of IONPs in PLGA NPs will be discussed in detail.

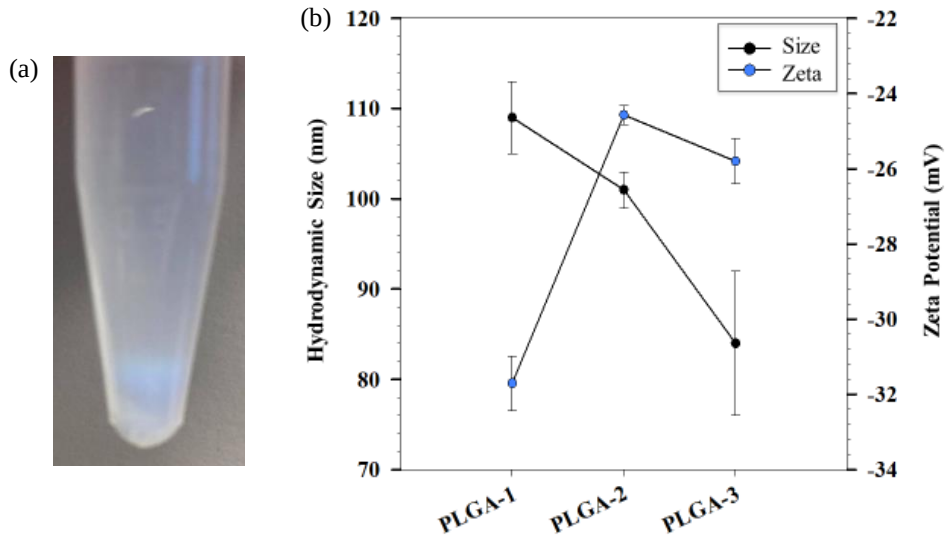

Figure 17: (a) Image of PLGA NPs settled at the bottom and (b) graphical representation of hydrodynamic size and zeta potential of bare PLGA NPs

4.2 Preliminary Optimization studies for encapsulation of IONPs by PLGA

4.2.1 Magnetic Separation Optimization

After the synthesis of bare PLGA NPs, PLGA-MAG NPs were synthesized by the method discussed in section 2.2.4. As seen evident from the results in previous section that effect of the molecular weight on the NPs size. Due to the minimal effect of molecular weight on NPs size only PLGA-1 (lowest molecular weight) was opted for further studies. After encapsulation of the IONPs, the polymeric nanoparticles become magnetic and can be easily retrieved by using a magnet. In order to retrieve all the magnetic PLGA-MAG NPs, the separation time on the magnet must be optimized. The process of IONPs encapsulation by PLGA NPs is not optimized. There is a possibility that three different populations of PLGA-MAG NPs, bare PLGA and free IONPs are present in the samples. For this purpose, three different studies were conducted in order to optimize the

magnetic separation time and retrieve all the PLGA-MAG NPs. Investigate the presence of three different populations.

In the first study (M1), three different batches of magnetic polymeric NPs were synthesized varying the initial IONPs concentration in the solvent phase. The amount of IONPs used in this study was 2,3 and 4 mg. Three batches for each amount of IONPs encapsulated PLGA NPs were synthesized and kept on the magnet for 2, 3 and 5 mins, respectively. The samples were then characterized using zeta sizer to estimate the hydrodynamic size. The plot for this study at different amounts of IONPs and different times is presented in figure 19 (a).

It can be observed from the figure 19 (a) that all the hydrodynamic sizes are in the range of 450 to 750 nm except for one sample at 3 mins time and 4 mg IONPs amount. In all the cases variation in the NPs size is seen and no probable trend is observed. This could be because, each batch of specific amount of IONPs is synthesized for a particular magnetic separation time. Maybe the NPs formed in all three experiments (of specific amount of IONPs) for different magnetic separation times have different size distribution of NPs in the particular batch. Also, the parameters like PLGA amount and amount of IONPs are not optimized so while separation of PLGA-MAG NPs, free magnetite can also be obtained which can change the NPs size obtained by zeta sizer.

Hence to overcome this challenge, another study (M1-1) was performed. In this study, each batch with 21 ml volume of specific IONPs amount i.e., 2, 3 and 4 mg encapsulated by PLGA NPs was divided into three samples of equal volume (7ml). These three samples of specific IONPs amount were kept on the magnet for 2,3 and 5 mins. The samples were then analyzed by zeta sizer to obtain hydrodynamic size of NPs. The graph for this study is presented in the figure 19 (b). It is evident from the graph that all the NPs size obtained are in the range of 250 to 350 nm. This could be because of the uniform distribution of NPs in each of the sample. Here it is also observed that the magnetic separation time did not have much impact on the NPs size. Hence it can be concluded that keeping the sample on magnet for two minutes will separate all the NPs and it is also evident from the image shown in figure 18 that the supernatant obtained after two minutes is clear.

Figure 18: Image of clear supernatant after 2 minutes of magnetic separation.

Another study (M1-2) was performed to optimize the magnetic separation time and also try to identify the population of PLGA-MAG NPs and free uncoated IONPs. In this study, the batch synthesized for each PLGA-MAG NPs with amount of 2, 3 and 4 mg was kept on the magnet for 30 seconds but while pipetting out the supernatant, the total magnetic separation time was estimated to be 45 seconds. The supernatant obtained for each batch was divided into three samples and kept for magnetic separation of 2, 3 and 5 mins. The reason for first 45 seconds separation was to separate free uncoated IONPs from the PLGA-MAG NPs and to confirm our hypothesis about the presence of different populations. The graph for this study is plotted and presented in figure 19 (c). It is evident from the graph that for three different PLGA-MAG NPs amounts, in first 45 seconds large NPs above 1µm are obtained. This is probably because of the magnetic aggregation of free IONPs which are not encapsulated into PLGA NPs. Since the IONPs surface is not functionalized with capping agents hence they can easily aggregate under the influence of external magnetic field because of their own magnetic dipole interactions.[82] Due to this reason, bigger NPs size is obtained in this case.

In case of 2 and 4 mg PLGA-MAG NPs, similar NPs size was obtained for 2, 3 and 5 mins magnetic separation while in case of 3 mg IONPs encapsulated PLGA different sizes for different magnetic separation times were obtained. This could be because of the non-homogeneous distribution of NPs while division into three batches. It can be concluded from the study that magnetic separation time did not have much impact on the NPs size and also the 45 seconds magnetic separation is beneficial for separating the uncoated IONPs. Although, in this study some results indicate the presence of free IONPs, still there is a need of a complete study in order to understand the presence and distribution of different populations in PLGA-MAG NPs samples. PLGA. Hence a study is presented in the next section. A table below also shows the difference in size of NPs obtained for these three studies and the possible reasons of size difference are also mentioned.

In all the three studies done for optimization of magnetic separation time only in the first study, an appreciable change in the NPs size was obtained probably because of the different size distribution of NPs in each batch while in other two studies, magnetic separation did not have much impact on the NPs size and hence it can be concluded from this that 2 minutes of magnetic separation is enough to separation the NPs from the supernatant and this is also evident from the image taken for two minutes magnetic separation.

Table 2: represents the summary of three studies including procedure and possible explanation for difference in sizes.

Method	Procedure	Sample	Size (nm)	Std	Reason for size difference
M1	Full batch magnetic separation for 2,3 and 5 mins	M1 (P-I-2)	559	9	Non-homogeneous distribution of sample
M1-1	Batch division into 3 parts and then magnetic separation for 2, 3 and 5 mins	M1-1 (P-I-2)	333	21	Homogeneous distribution of sample but with free IONPs
M1-2	Full batch magnetic separation for 45 seconds then division into 3 parts for 2,3 and 5 mins magnetic separation	M1-2 (P-I-2)	673	99	Separation of free IONPs but large size might be because of some left aggregated IONPs

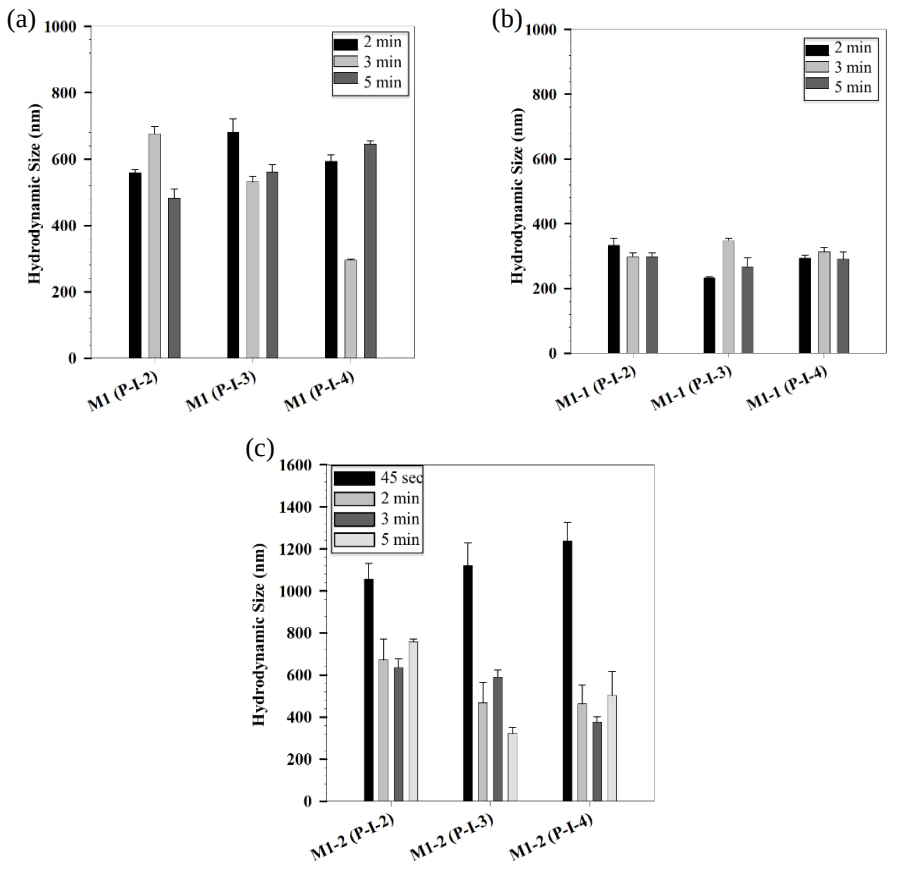

Figure 19: Graph represents the hydrodynamic size of NPs at different IONPs concentrations and at different magnetic separation times in study in (a) M1, (b) M1-1, and (c) M1-2.

4.2.2 Identification of populations of NPs

The main aim of this study was to optimize magnetic separation time and to see the particle size distribution in short intervals of magnetic separation. Since the process of obtaining PLGA-MAG NPs is not optimized. It is believed that there might be presence of different populations of NPs i.e., bare PLGA, free magnetite and PLGA-MAG NPs as shown in figure 20.

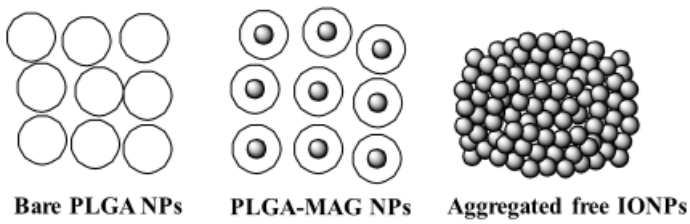

Figure 20: Illustration of three different populations possibly present in samples.

So, a methodology was developed to identify the different populations of PLGA-MAG NPs, bare PLGA and free aggregated IONPs by first centrifuging the sample and then step wise separating the NPs with a magnet in four short intervals of 30 seconds.

Right after the synthesis process, the solution (21 ml) containing the three particle populations, was divided into two parts and PLGA encapsulated IONP at a specific concentration of 4 mg was centrifuged for 2 and 5 mins. Then the samples were kept on magnet for 30 seconds (denoted as B1 in the graph). The bottom product (B.P) of B1 was then redispersed in 7 ml MQ water and kept for characterization. The top product (T.P) (which was the supernatant of B1) was again kept on magnet for 30 seconds denoted as B2. The same process as mentioned above for both samples (centrifuged sample for 2 and 5 mins) was repeated for two more times represented as B3 and B4. A schematic of this methodology is presented in the figure below:

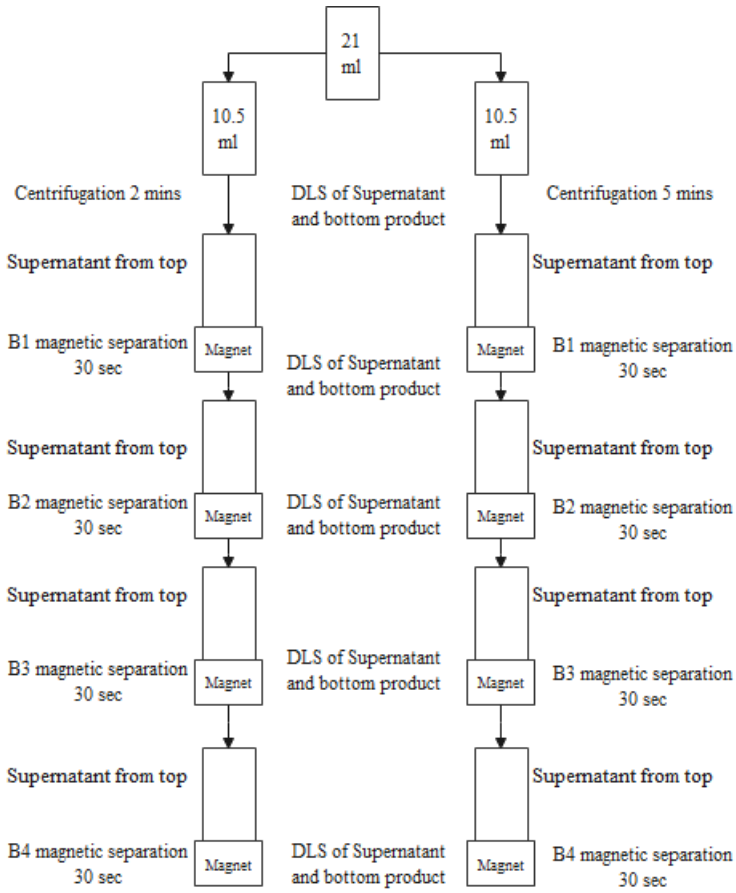

Figure 21: Methodology to identify various populations in sample.

It is evident from the graph in figure 23 that, the samples centrifuged for 2 and 5 mins had a similar size in the range of 780-800 nm. Since the samples are centrifuged so there would be presence of most likely three populations that include PLGA-MAG NPs, free PLGA NPs and free aggregated IONPs. Also, after the centrifugation a colourless supernatant was obtained with a pellet of NPs at the bottom. This colourless supernatant confirms that all the NPs has settled down. Furthermore, centrifugation at 14500 rpm and for 2 to 5 mins has shown the NPs size around 90 nm. A similar hydrodynamic size for aqueous Pluronics F-127 was obtained which means only the surfactant is left in the sample after

centrifugation. The presence of all these populations could be a possible reason for a bigger particle size detected by zeta sizer.

The sample kept for first 30 sec magnetic separation (B1) had the largest particle size in the range of 1150-1250 nm (represented as legend 2 in figure 23). This separated fraction could be the aggregated IONPs that has not been coated with PLGA. It must be noted that the magnetite used in this work has no specific capping agent, except hydroxy groups on the surface as reported by Dave et al.[83] Thus, when the solution above is placed on a magnet, these free IONPs may aggregate due to magnetic forces among them and precipitate out as the first fraction. A similar aggregation phenomenon was also observed by Ezzaier et al.[89]

In B2 separation (represented as legend 3 in figure 23) for both samples centrifuged for 2 and 5 mins, different sizes were obtained. For the sample centrifuged for 2 mins, in process B2, smaller size in range of 500 nm was obtained while for 5 min centrifuged sample, the size was above 700 nm. Larger size in the second case (B2-5 min centrifugation) could be because of some left-over IONPs aggregates in the sample. While smaller size in first case (B2-2 min centrifugation) represents the population of PLGA-MAG NPs. Polydispersity Index (PDI) for both cases represent the difference in the size obtained in the zeta sizer instrument. It was observed that the PDI for case one (0.5) is less than that in case two (0.65). This gives an idea that in case two, a polydisperse population is present compared to case one.

In case of B3 and B4, similar size was obtained in both samples and compared to separation step B1, the size obtained was quite small in the range of 350-500 nm. In the case of B3 and B4, it is believed that there is only presence of PLGA-MAG NPs. From these results it can be concluded that in the first magnetic separation B1, the free magnetite is separated from the samples and then in the other steps encapsulated magnetite is separated as a B.P. As evident from the size which decreases with separation from B1 to B4, it can be inferred that all the PLGA-MAG NPs are separated and only free PLGA and those PLGA-MAG NPs might be left in the supernatant which had a low magnetization.

A proof of presence of two populations of free IONPs and PLGA-MAG NPs was obtained by HR-TEM images presented in figure 22. PLGA-MAG NPs with specific concentration of 4 mg were analyzed under HR-TEM before magnetic cleaning and it was observed that free aggregated IONPs are also present along with PLGA coated IONPs. The reason is due to the unoptimized process.

(a) (b)

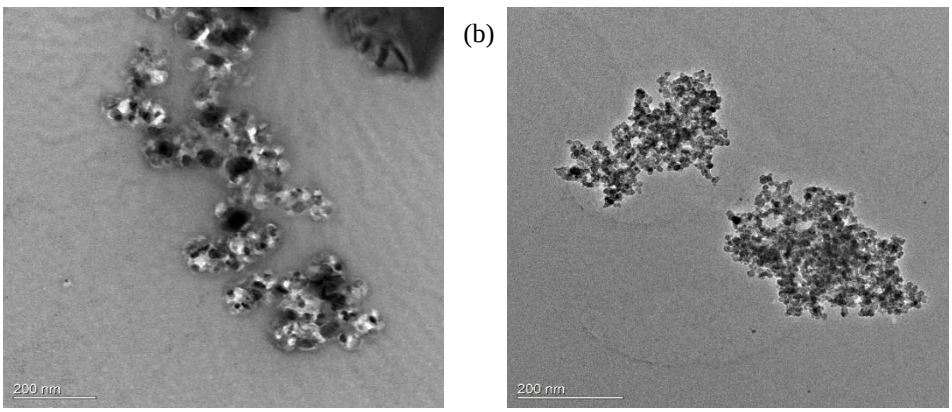

Figure 22: HR-TEM images of 4 mg IONPs encapsulated by PLGA. Here represents the population of (a) PLGA-MAG NPs and (b) free aggregated

Similar studies were also performed for 0.5 and 2.0 mg IONPs encapsulated in PLGA and the trends obtained for both cases were quite similar to the results explained above. The graphical representations are attached in the Appendix A.

Hence, in this study, an understanding of presence of different NPs populations was acquired and proved to some extent. But there is still need of more studies to evidently conclude about this hypothesis. In the next section, a study to optimize the mixing process of IONPs with PLGA and DMSO will be discussed in detail.

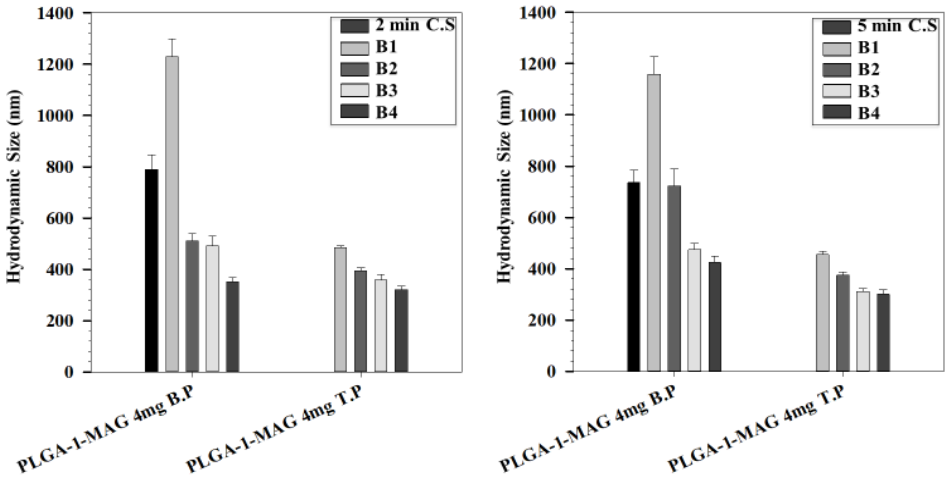

Figure 23: Plot represents the data obtained for different magnetic separation steps explained in the methodology presented in Figure 21.

4.2.3 Effect of mixing of IONPs with PLGA/DMSO mixture on size of PLGA-MAG NPs

In this study, PLGA-MAG NPs were synthesized at different IONPs concentrations i.e., 0.5, 1 and 2 mg. The magnetic separation was first done for 45 seconds and then the batch of 21 ml sample was divided into three and further magnetically separated for 2,3 and 5 mins, respectively. During the initial experiments, the mixing of IONPs with PLGA and DMSO mixture was not time based and these three components were not mixed for a particular amount of time. The results for the initial experiments are presented in figure 24 (a).

It is evident from the graph (figure 24 (a)) that in initial experiments, the size obtained for 0.5, 1 and 2 mg concentration IONPs for PLGA-MAG NPs in 45 seconds magnetic separation is in the range of 1000-1200 nm, this could be because of the free aggregated IONPs obtained as explained and discussed in section 4.2.1. The NPs size obtained for 2 min magnetic separation had decreasing trend with increasing amount of IONPs. The

NPs size decreased from 950 to 450 nm with increased amount of IONPs from 0.5 to 2 mg. A similar decreasing trend for NPs size was also observed for 3 and 5 mins magnetic separation. The NPs size decreased from 850 to 400 nm in 3 mins magnetic separation and 780 to 550 nm in 5 mins magnetic separation, respectively. Another notable point is that in 5 min magnetic separation for 1 mg IONPs concentration, the size was smaller than 2 mg IONPs. This trend was observed to be different from the rest of the results obtained. The trend obtained in these initial experiments could be because IONPs were not well mixed in the PLGA/DMSO solution which will result in uneven distribution of IONPs across the mixture and they might have aggregated NPs which will result in different populations of particles.

Since the mixing process of IONPs with PLGA/DMSO was not time based. So, a study was conducted in which the mixing step was optimized by mixing the IONPs with PLGA/DMSO and vortexing the mixture for 10 secs in three steps. It was found that a different NPs size trend compared to initial experiments was obtained after the optimization of this process.

As evident from the graph in figure 24 (b), an increasing trend of NPs size is observed while increasing the IONPs concentration. The free aggregated IONPs for three different concentrations of IONPs were separated in first 45 second separation. The size of the aforementioned aggregated IONPs was obtained to be in the range of 600-1400 nm. In 2 min magnetic separation with increasing amount of IONPs for PLGA-MAG NPs synthesis, the NPs size was increased from 400 to 750 nm. The NPs size increased from 500 to 750 nm and 520 to 800 nm, respectively for 3 and 5 mins magnetic separation. The increasing trend of PLGA-MAG NPs could be because of the fact that increased number of IONPs are being encapsulated by PLGA. Also, before encapsulation by PLGA the IONPs can aggregate with each other because they do not have capping agent on their surface. If aggregated IONPs are being encapsulated by PLGA than the size of PLGA-MAG NPs can substantially increase.

After this optimization of mixing process, a similar trend was observed in all the experiments performed using the same methodology. This optimization step has found to be vital in this process, because if the IONPs are not mixed well in the PLGA/DMSO solution then the non-

homogeneity in the solution will affect the encapsulation of IONPs in PLGA NPs. The IONPs can aggregate due to non-homogeneous mixing and a deviation in NPs size would be observed in all the experiments while homogeneous mixing of IONPs will reduce the chances of aggregation and hence encapsulation of IONPs will be better and homogeneous. After this optimization step, similar trend was obtained in all the experiments performed.

Hence in this study, the mixing process of IONPs with PLGA and DMSO was optimized for the reproducibility of the experimental results and better encapsulation of IONPs with PLGA. In the next study, the effect of IONPs batch concentration on the size of PLGA-MAG NPs will be discussed in detail.

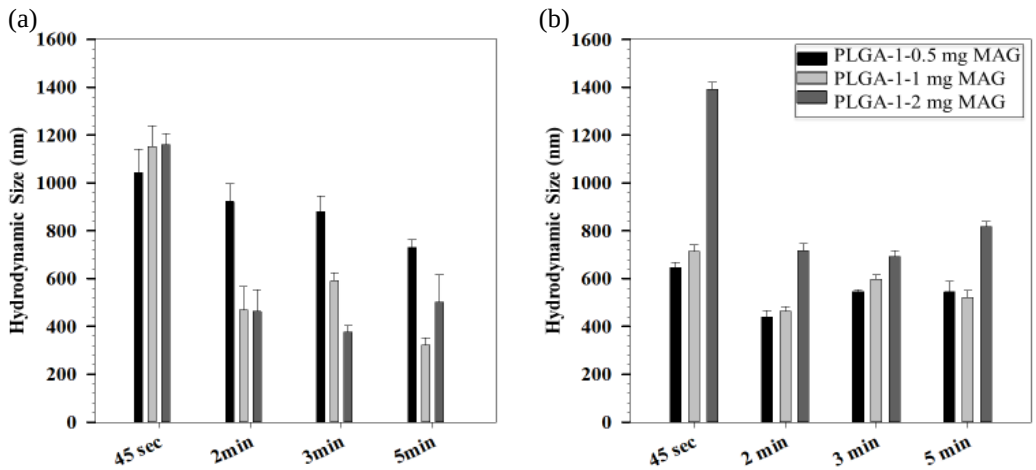

Figure 24: Plot representing the hydrodynamic size at different separation times and different IONPs concentrations encapsulated by PLGA in (a) initial experimental study and (b) after optimizing mixing process of IONPs with PLGA/DMSO mixture.

4.2.4 Effect of IONPs batch concentration on the size of PLGA encapsulated IONPs by Nanoprecipitation

In all the preliminary studies before this study, IONPs with stock concentration of 57 mg/ml were used. A variation in the concentration of IONPs batch stock was studied at three different concentrations i.e., 5, 25 and 57 mg/ml in order to investigate the influence of batch concentration on the size of NPs. The main reason was that if a higher concentration batch i.e., 57 mg/ml is used then for lower amounts like 0.5 mg of IONPs approximately 9 µl of sample has to be pipetted out. While pipetting out such small amounts, the error in the volume measurement will increase to a higher extent. Hence, due to this difficulty of accurate volume measurement of IONPs. Different PLGA-MAG NPs sizes might be obtained because of different batch concentrations of IONPs. In this study, PLGA-1-MAG NPs at different initial concentrations of IONPs i.e., 0.5 mg, 2 mg, and 4 mg, respectively were synthesized.

As evident from figure 25 (a), for 5 mg/ml IONPs batch concentration, the PLGA-MAG NPs size increased from 362 to 638 nm which is 28 % increase in NPs size. In case of 25 mg/ml batch concentration, the encapsulated NPs size increased from 497 to 665 nm, which is 14 % increase in NPs size. Similarly, in case of 57 mg/ml batch concentration, 483 to 767 nm which is 23 % increase in NPs size. An increasing NP size trend was observed in all the cases. Hence it is evident that increasing the batch concentration of IONPs has affected the size of NPs. Also, with increasing the amount of IONPs from 0.5 to 4 mg, an increase in NPs size is observed in all the experimental results at different IONPs batch concentrations.

One of the reasons could be that since IONPs surface is not functionalized, the IONPs can aggregate easily because of dipolar magnetic forces.[89] The increased concentration of IONPs can promote the process of aggregation. Hence, at a higher batch concentration aggregated IONPs are present and they result in increased size of NPs after encapsulation in PLGA. To ensure the reproducibility of the results, the same experiments were repeated three times at 5 and 57 mg/ml batch concentration using

IONPs concentration of 0.5, 2 and 4 mg. The experiments were reproduced three times and the reproducibility data is attached in the appendix as a graphical representation.

Hence from this study it can be concluded that the IONPs batch stock concentration can influence the size of the NPs formed. Lower concentration of IONPs batch should be used in order to ensure homogeneous separation of IONPs from the batch. Also, it will ensure the reproducibility of the results.

In the upcoming study, a screening design was made in JMP software, in order to study the effect of different parameters on NPs size. For experimental design in JMP software, the PLGA-MAG NPs were first kept for 45 seconds on the magnet and then divided into three batches of equal volumes. One out of three batches was kept on the magnet for two minutes and characterized using zeta sizer. The IONPs stock concentration of 5 mg/ml was used.

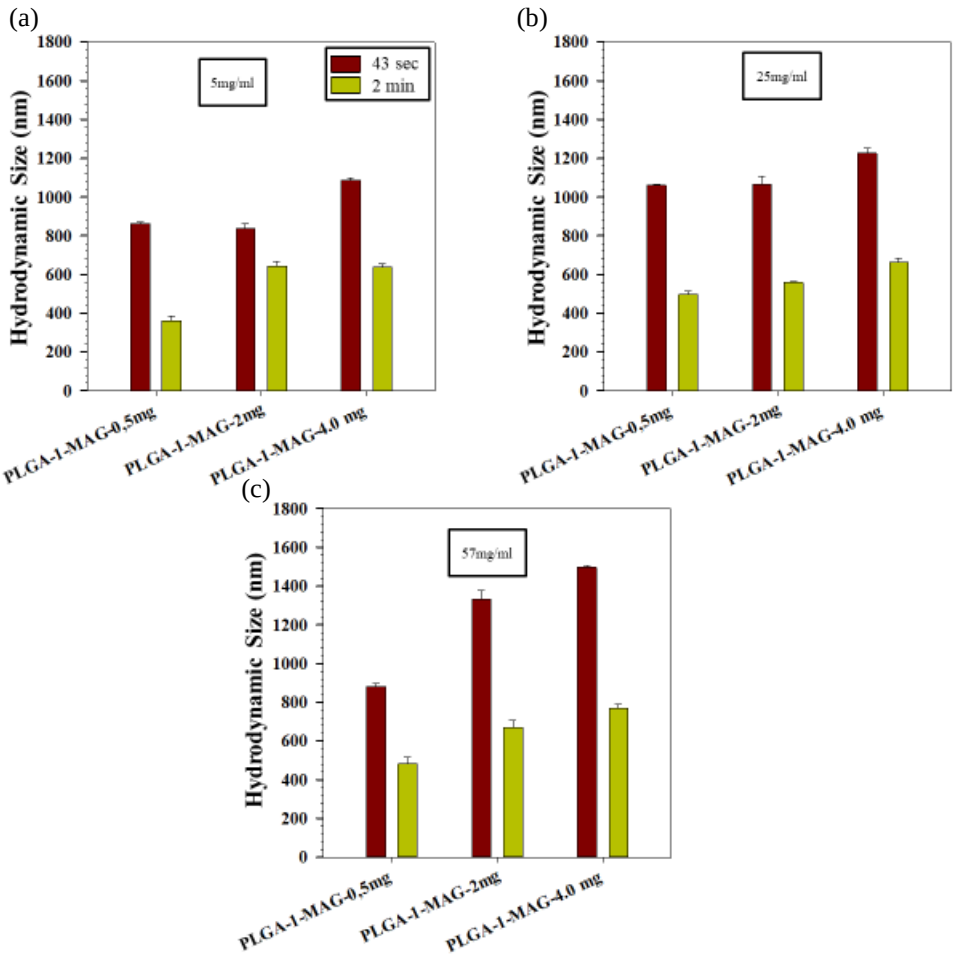

Figure 25: Plot representing the hydrodynamic size obtained at different IONPs concentrations encapsulated by PLGA (a) At IONPs batch concentration of 5 mg/ml, (b) at IONPs batch concentration of 25 mg/ml, and (c) at IONPs batch concentration of 57 mg/ml.

4.3 Design of experiment in JMP software

4.3.1 Parameters study 1

A two level screening design was made in JMP software, in order, to study the effect of molecular weight, polymer/IONPs ratio, aqueous/organic ratio, and injection rate of solvent phase on the size of PLGA-MAG NPs. The design of experiments is attached in appendix C. In this design, the two polymers used are PLGA-1, having molecular weight 7000-17000 Da and PLGA-3, with molecular weight of 30000-60000 Da. The polymer/IONPs (weight/weight) ratio was fixed at 7.5 and 20, the aqueous/organic ratio (volume/volume) was set to 5 and 20 and the injection rate of solvent phase was maintained at 4.5 and 14.5 ml/hr.

In case of fixed molecular weight, a decreasing NPs size trend was obtained while increasing the polymer/IONPs ratio. For PLGA-1 and 7.5 polymer/IONPs ratio, the NPs size obtained was in the range of 700 nm (in figure 26 (a)) while increasing the ratio to 20 caused a decrease in the size up to 450 nm (in figure 26 (b)). In case of 7.5 polymer/IONPs ratio, the amount of PLGA and IONPs used is 30 mg and 4 mg respectively, while in case of 20 polymer/Fe ratio, the amount used for PLGA is 10 mg and 0.5 mg for IONPs. At polymer/IONPs ratio of 7.5 for PLGA-3, the PLGA-MAG NPs size was obtained in the range of 400 nm while at polymer/IONPs ratio of 20 it was obtained to be in the range of 300 nm.

The other trend which is evident in the graph (in figure 26) is the decrease of NPs size with the increase in molecular weight. At a fixed polymer/IONPs ratio of 7.5, NPs size obtained for PLGA-1 is in the range of 700 nm while for PLGA-3 it is in the range of 350 nm. In case of fixed polymer/IONPs ratio of 20, 450 nm NPs size range was obtained for PLGA-1-MAG NPs while for PLGA-3-MAG NPs, the range was around 300 nm. Statistically, the data obtained from the experiments for PLGA-1 and PLGA-2 at polymer/IONPs ratio of 7.5 has a lower standard deviation and variation in the data set compared to the data obtained in case of 20 polymer/IONPs ratio.

Variation in the aqueous/organic ratio and injection rate did not have much impact on the NPs size as evident from the graph (in figure 27 (a) and (b)) obtained. According to literature, in most of the studies, these two factors have different trends depending on the studies. In section 1.4.2, a study is illustrated where Budhian et al.,[64] did not observe any change in the NPs size while changing the aqueous/organic ratios. While another study showed a decrease in NPs size with increasing the aqueous/organic ratio.[63]. The reason was the decrease in viscosity of the system which will result in smaller NPs. Here in our case, the aqueous/organic ratio was changed in the non-solvent phase by adding DMSO into aqueous pluronics F127 mixture. If the DMSO was changed in the solvent phase containing PLGA and IONPs, similar trends would have been observed as described above. In both of the above-mentioned studies, bare PLGA NPs were formed without encapsulation of IONPs.

Injection rate influence was also reviewed in literature, Xie et al.[90] studied the effect of injection rate on the size of PLGA NPs and they found that increasing injection rate decreases the NPs size significantly. While in our case, the injection rate did not have significant impact on the NPs size. This could be because, the injection rate used in our case is 4.5 and 12.5 ml/hr while in the study mentioned above has the injection rate of 35 to 80 ml/min which is much higher than our case. Hence, it can be inferred that the injection rate has to be increased significantly in order to see a change in the NPs size.

After completion of this design, it was found that the R^2 for this experimental design was obtained to be 0.84. In this design, backward selection of least significant variable was done. In backward selection those variables which have higher significant value are eliminated from the design in order to obtain the least significant variable. Hence, by backward selection of the least significant variable in this design it was found that the molecular weight and polymer/IONPs ratio has the least significant value which means these parameters had the largest effect on the data set obtained. Also, aqueous/organic ratio and injection rate had the least effect on the data set, since a high significant value was obtained. The values for these parameters are shown in table 3.

From this study, it was concluded that the molecular weight and polymer/ratio are the important parameters. A three level screening design was made considering the above mentioned parameter. The study is discussed in the next section.

Table 3: Summary of model fit for study 1.

Summary of Fit	
RSquare	0.836007
RSquare Adj	0.776373
Root Mean Square Error	86.92973
Mean of Response	435.1625
Observations (or Sum Wgts)	16

Table 4: Summary of parameter estimates for study 1.

Parameter Estimates	
Term	**Prob> t**
Intercept	<.0001*
Aqueous/Organic ratio (5,20)	0.9203
Injection rate (4.5,13.5)	0.5885
Molecular Weight (13000,45000)	<.0001*
Polymer/IONPs ratio (7.5,20)	0.0015*

(a) (b)

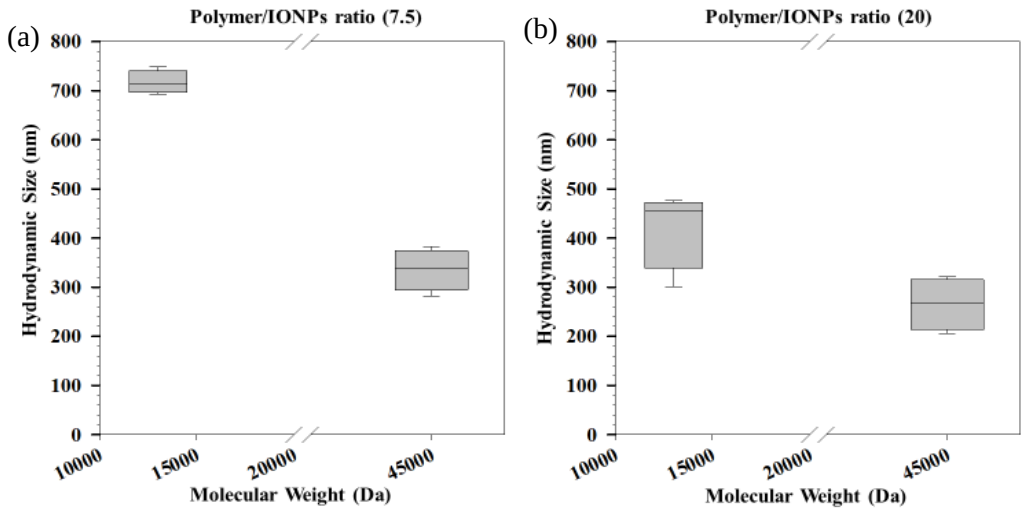

Figure 26: Hydrodynamic size relationship between Polymer/IONPs ratio and Molecular weight. (a) at polymer/IONPs ratio 7.5 and (b) at polymer/IONPs ratio 20

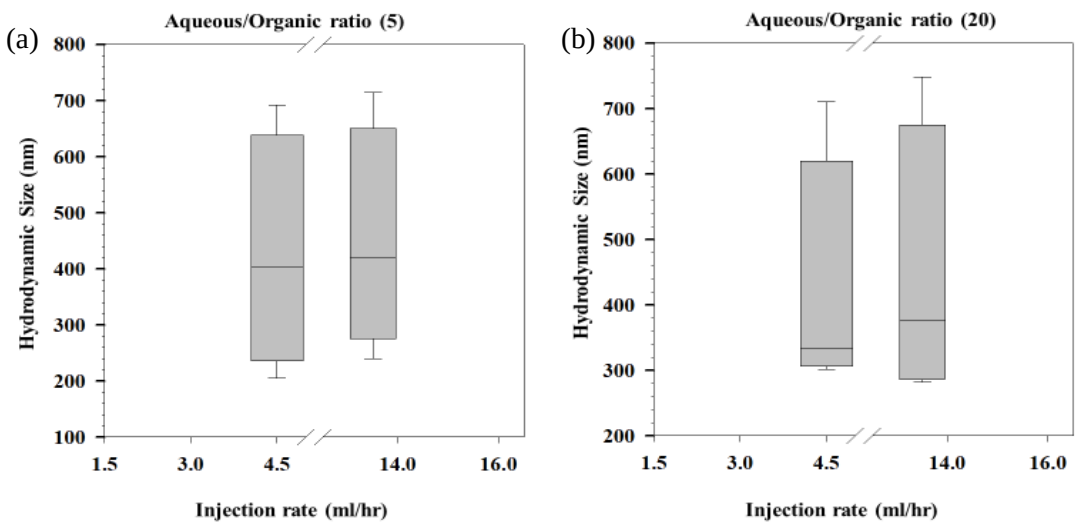

Figure 27: Hydrodynamic size relationship between aqueous/organic ratio and injection rate. (a) at aqueous/organic ratio 5 and (b) at aqueous/organic ratio 20

4.3.2 Parameters Study 2

As discussed in the previous study that the molecular weight and polymer/IONPs ratio had the largest effect on the data set. So, in this study, the Polymer/IONPs ratio was treated as two parameters along with molecular weight. Each of the parameter is studied at three different data points i.e., polymer amount at 10, 20 and 30 mg, IONPs amount at 0.5, 2 and 4 mg and molecular weight at 14000, 31000 and 45000 Da. The design of experiments is presented in the Appendix C as figure C.2

Table 5: Presents the quantity and the parameters that are studied in study 2.

Parameter	Quantity
Molecular Weight	14000,13000 and 45000 Da
Amount of IONPs	0.5, 2 and 4 mg
Amount of PLGAs	10, 20 and 30 m

In case of molecular weight, it was observed that a decrease in NPs size was obtained with increasing the molecular weight from 14000 to 45000 Da. A similar trend was also observed in the previous study in section 4.3.1. At 0.5 mg IONPs and 10 mg polymer amount, varying the molecular weight from 14000 to 45000 had a decrease in NPs size from 325 to 250 nm while increasing the IONPs amount to 4 mg and keeping polymer amount at 10 mg, with increase in molecular weight the NPs size reduced from 580 to 373 nm.

If a comparison is made based on percentage decrease in NP size, then in the second case the NPs size decreased by 21% while in case one it decreased by 13%. A similar trend of decreasing NP size with increasing molecular weight was also observed while increasing the amount of polymer to 20 and 30 mg and keeping IONPs amount at 0.5 and 4 mg. For 20 mg polymer at 0.5 and 4 mg IONPs, increasing the molecular weight decreased the NPs size by 12% and 32% respectively. In case of 30 mg polymer at 0.5 and 4 mg IONPs, the highest percentage decrease was obtained i.e., 28 % and 37% respectively with increased molecular weight.

The amount of polymer has also impacted the size of NPs. In case of 14000 M.W at 0.5 and 4.0 mg IONPs amount, increasing the amount of polymer from 10 to 30 mg increased the NPs size from 325 to 572 nm and 580 to 731 nm, respectively. Similarly, with 31000 M.W and same IONPs amounts, surging amount of polymer increased the NPs size from 329 to 404 nm and 560 to 680 nm, respectively. At the highest M.W and similar IONPs amount as mentioned above, the NPs size increased from 250 to 322 nm and 373 to 395 respectively with polymer amount increment.

Another interesting trend observed in the results explained above was that the increase in NPs size with increasing polymer amount reduced with increase in molecular weight. For instance, the increment in NPs size difference in case of 14000 M.W for both 0.5 and 4.0 mg IONPs amount was averaged to be 199 nm with increasing polymer while in 45000 M.W and same IONPs amount the difference in NPs size was averaged to be 57 nm. So, the increment in size for lowest M.W is four times less than the highest M.W.

Another parameter that was studied is the amount of IONPs used. It is evident from the graph, that increase in IONPs amount has increased the NPs size in all the different amounts of polymer and M.W. However, in all the cases variation in the increase of NPs size has been observed.

For 14000 and 31000 M.W, the increment in NPs size with increasing amount of IONPs is much more than the NPs size obtained for 45000 M.W. For example, the percentage increase in NPs size for 14000 M.W at 10 mg polymer amount is 28% while for same polymer amount but 45000 M.W, the increase is 19%.

The R^2 for this experimental design was obtained to be 0.83 which indicates that the model is good enough to predict the most important parameter that affects the data set significantly. In this set of experimental design, molecular weight, and the amount of IONPs used are found to be the most important parameters that affect the size of the NPs size. Hence varying these two parameters will significantly change the NPs size.

The results obtained in the JMP design 1 and 2 will be discussed in detail with reference to literature in the following paragraph:

The supersaturation leading to polymer precipitation is generated because of the diffusion of solvent into the non-solvent phase exposing the polymer to the aqueous phase. When the amount of polymer is increased the supersaturation of the polymer in the non-solvent (water) will also increase. An increase in supersaturation will increase the nucleation rate resulting in larger number of smaller NPs. However, an increased polymer concentration represents increase in number of polymer chains, leading to higher probability of aggregation. Thus, bigger NPs have been reported in literature when it comes to synthesis of bare polymeric NPs. Hernandez-Giottonini et al. [62] observed a similar trend of increasing NPs size with increasing the PLGA concentration from 5 mg/ml to 15 mg/ml. The bare PLGA NPs size obtained for 5 mg/ml and 15 mg/ml PLGA concentration was 157 ± 9 and 194.5 ± 2.6 nm, respectively. Although they have used different surfactant i.e., PVA and different solvent i.e., Dichloromethane but similar trend of increasing NPs with increased polymer concentration was obtained. They provided the same reason as discussed above.

In section 4.3.1, an increasing PLGA-MAG NPs size was obtained when the polymer/IONPs ratio was changed from 20 to 7.5. This is probably because, in 7.5 ratio of polymer/IONPs, 30 mg of PLGA and 4 mg of IONPs are present compared to 10 mg of PLGA and 0.5 mg IONPs present in polymer/Fe ratio of 20. An increased amount of PLGA can result in increasing the number of PLGA chains and higher probability of aggregation of PLGA NPs. Hence bigger PLGA-MAG NPs size is obtained in this case. In section 4.3.2, the amount of PLGA was varied from 10 mg/ml to 30 mg/ml and an increasing NPs size trend was observed. This could possibly be because of the above mentioned reason.

The encapsulation of hydrophobic drugs into PLGA NPs by nanoprecipitation has been reported by many researchers in literature. Hoda et al.,[91] also reported the encapsulation of disulfiram (hydrophobic drug) in PLGA NPs by nanoprecipitation. They studied the interactions of PLGA with disulfiram using different characterization techniques such as Raman spectrum analysis and isothermal titration calorimetry. After obtaining results from these characterization techniques, they suggested that the major interactions between PLGA and

disulfiram is probably because of hydrophobic-hydrophobic interactions compared to other interactions such as Van der Waal, Hydrogen bonding etc. The reason they gave was that according to their results, the polymer-drug interaction was entropy driven and hydrophobic interaction are entropy driven while Van der Waal and Hydrogen bonding are enthalpy driven interactions.

In our studies, we have tried the encapsulation of hydrophilic moiety i.e., IONPs into PLGA NPs. None of the research articles talk about the interaction of PLGA NPs with hydrophilic drugs or hydrophilic moieties. Also, a clear understanding of how hydrophilic moieties are encapsulated into polymer matrix is also missing in the literature. Hence, in this study, an attempt to describe the interactions between IONPS and PLGA has been made. It can be hypothesized that the encapsulation of IONPs inside the PLGA matrix is probably because of the fast mixing process than the diffusion of IONPs outside the PLGA matrix along with the solvent. If the mixing process is not fast enough then the IONPs will diffuse out of the solvent phase along with DMSO and no encapsulation of IONPs into PLGA will occur. Another hypothesis could that there are intermolecular interactions such as van der Waal interactions between IONPs and the polymer in the solvent phase. Due to these interactions, the precipitation of polymer will occur along with IONPs and the IONPs will be entrapped inside the polymer matrix. This is evident in figure 20 a where PLGA-MAG NPs with 4 mg concentration were imaged.

Increasing the concentration of IONPs in PLGA/DMSO mixture will increase the interactions between IONPs and PLGA. Hence, greater number of IONPs will be encapsulated inside the PLGA matrix and bigger NPs size will be obtained. The increasing PLGA-MAG NPs size trend was observed in section 4.3.2, where increasing the amount of IONPs resulted in increased NPs size, this could be because of the similar reason mentioned above.

The molecular weight of polymer can also greatly affect the NPs size. Increasing the molecular weight from 14000 to 45000 Da resulted in decreasing the size of PLGA-MAG NPs. This trend was observed in both the studies in section 4.3.1 and 4.3.2, respectively. If the molecular weight is increased in case of PLGA, the number of hydrophobic chains is increased in the polymer and if the hydrophobicity of the polymer is

increased, then the NPs will try to reduce the entropy of the system i.e., decrease the interactions with the water. This will result in formation of smaller NPs with increased molecular weight. Öztürk et al.[86] also observed a similar size decreasing with increase in molecular weight of PLGA but they synthesized bare PLGA NPs without encapsulating IONPs.

Table 6: Summary of model fit for study 2.

Summary of Fit	
RSquare	0.836558
RSquare Adj	0.81524
Root Mean Square Error	59.79598
Mean of Response	460.3185
Observations (or Sum Wgts)	27

Table 7: Summary of parameter estimates for study 2.

Parameter Estimates	
Term	**Prob> t**
Intercept	<.001*
Molecular Weight	<.001*
IONPs Amount	<.001*
Polymer Amount	0.0004*

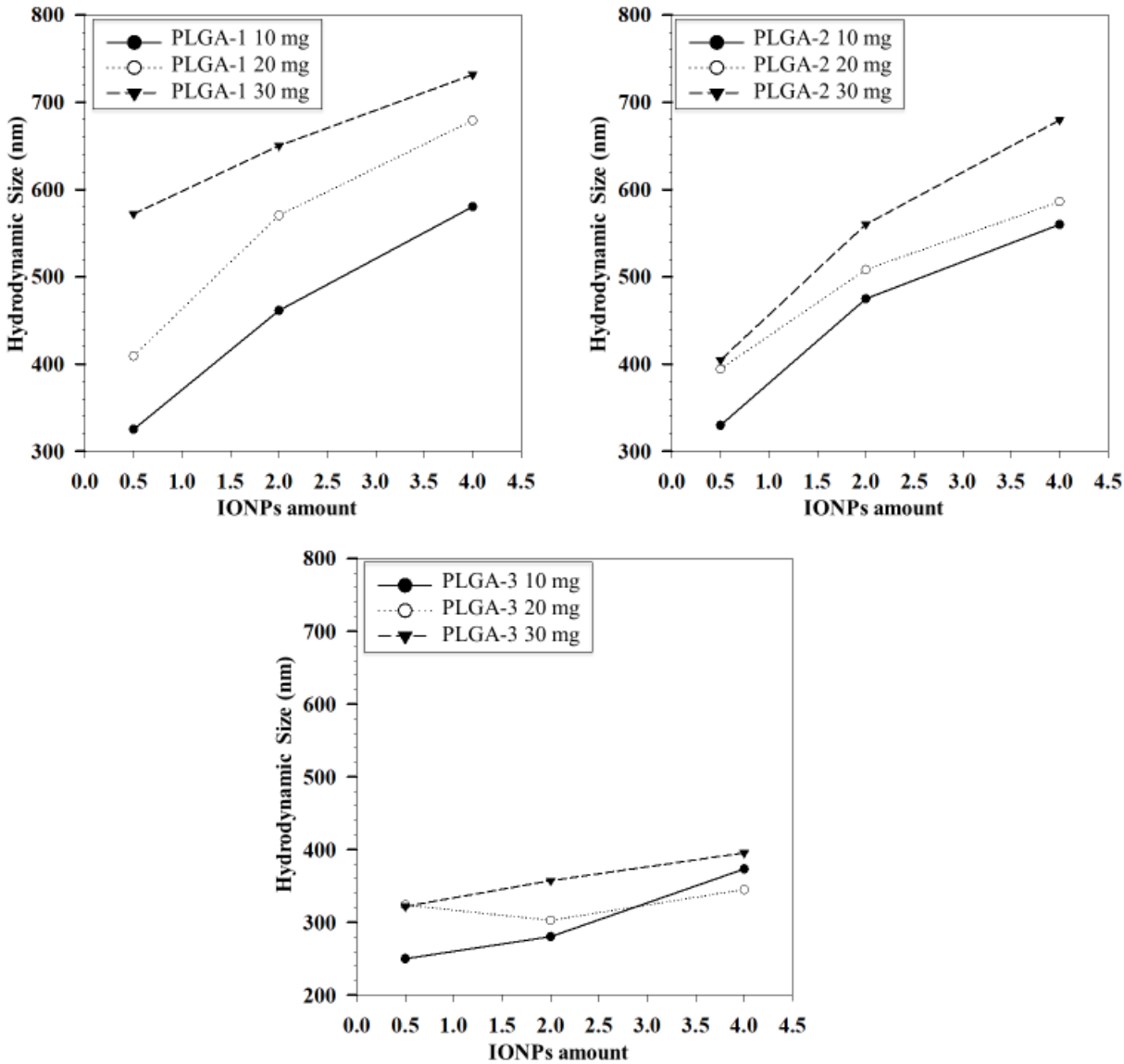

Figure 28: Hydrodynamic size relationship between IONPs and polymer amount at particular molecular weight of PLGA.

4.4 Drug loading with Coumarin

Coumarin which is a hydrophobic drug was loaded into PLGA-1 and PLGA-1 encapsulated IONPs by the method described in section 2.8 and 2.9. The drug calibration was done at various concentrations and a plot for the drug calibration is represented in figure 30 (a). The drug peak in the UV-Vis was obtained at a wavelength of 277 nm. Since the drug signal at a higher concentration was distorted because of the noise, so the values for concentration of coumarin were plotted in drug calibration curve from the point where noise in the signal was negligible. The graphical representation of curves obtained in UV-Vis at two different coumarin concentrations i.e., 0.5 mg and 0.0125 mg are presented in figure 31. It is evident that around 277 nm, there is a noise in the signal which makes it difficult to detect the 277 nm point while in lower concentration a prominent peak is visible at 277 nm. Due to this reason, the calibration curve was plotted at concentrations where the peak at 277 nm was distinctly visible. The slop of the calibration line was obtained to be 74.141 and this value was used while calculating the drug loading.

Another drug calibration was done in order to observe the interaction of pluronics F127 and coumarin shown in figure 30 (b). Since both of these are hydrophobic compounds, there might be some interaction between the surfactant and the drug after the addition of solvent phase containing the drug into the non-solvent phase containing pluronics F127 if the PLGA is unable to entrap the drug. The calibration plot for pluronics F127+coumarin is represented in figure 30 (b). The slope of the calibration line was 66.9. Although, there is a slight change in the slope of calibration line but still the drug signal was detectable at 277 nm wavelength which means that there is almost negligible interaction between the pluronics F127 and coumarin, otherwise the drug would not be detected at a close absorbance value.

For 0.5, 1.0 and 1.5 mg coumarin loading in PLGA NPs, the drug loading efficiency was obtained to be 85, 90 and 91 % respectively. It was observed that by increasing the amount of drug, the drug loading efficiency increased by 6 %. This means that the PLGA NPs can encapsulated more drug until they are saturated with drug. Although, 1.5

mg was the highest concentration of drug used but increasing the drug amount might provide more drug loading efficiency.

The hydrodynamic size for drug encapsulated PLGA NPs was obtained to be 102 ± 3, 100 ± 2 and 108 ± 1 nm for 0.5, 1.0 and 1.5 mg drug concentration. For bare PLGA, the hydrodynamic size was obtained to be 104 nm, but it was observed that a smaller NPs size was obtained in case of 0.5 and 1.0 mg drug concentration, this could be because of the increased hydrophobicity of the NPs. Since the drug is being entrapped inside the PLGA matrix, the hydrophobicity of the system containing the PLGA and coumarin will increase which will result in formation of smaller NPs in this case. While in case of 1.5 mg drug concentration, the bigger NPs size obtained could be because of the saturation of PLGA NPs with the drug.

PLGA-MAG NPs with amounts of 0.5 and 4.0 mg were also loaded with coumarin using three different amounts i.e., 0.5, 1.0 and 1.5 mg, the drug loading efficiency is tabulated in table 8. It was found that the drug loading efficiency did not significantly decreased in this case where IONPs were also present in the PLGA matrix. For 0.5 mg IONPs encapsulated by PLGA NPs compared to PLGA loaded coumarin NPs, the drug loading efficiency decreased by 3 % for 0.5 mg coumarin while for 1.0 and 1.5 mg coumarin the decrease in drug loading was just 2 and 1% respectively.

On the other hand, increasing the IONPs content had also affected the drug loading efficiency to some extent. For 4 mg IONPs encapsulated by PLGA NPs at 0.5 mg coumarin compared to PLGA loaded coumarin NPs, the drug loading efficiency decreased by 4 % and for same IONPs at 1.0 and 1.5 mg coumarin amount, the decrease was obtained to be 2% in both cases. The decrease in drug loading efficiency could be because of the entrapment of IONPs together with the drug inside the PLGA shell. Since two moieties are being encapsulated inside polymer shell so a point will come where the PLGA shell will be saturated with moieties and further uptake of drug will not be possible. This was also observed when the amount of IONPs was increased the drug loading decreased.

The hydrodynamic sizes of coumarin loaded IONPs/PLGA NPs were also obtained using zeta sizer and the plot of those is available in the figure 29. It is evident from the graph that a decrease in NPs size was obtained while

increasing the amount of drug. Another trend which was observed was the increase in NPs size with the increased amount of IONPs. The decreasing NPs size with increased coumarin amount could be because of the increase in hydrophobicity of the NPs. The coumarin and polymer will have hydrophobic-hydrophobic interaction and hence, increased amount of drug will increase the hydrophobicity of the solvent phase hence smaller NPs are obtained. This phenomenon has also been explained by Hoda et al.,[92] where they studied the interactions between the hydrophobic drug i.e., disulfiram and PLGA. Based on their results, they suggested that PLGA and hydrophobic drugs have hydrophobic-hydrophobic interactions as major interaction. This is also explained in section 4.3.2. Also, increasing the amount of IONPs could increase the NPs size because a greater number of IONPs will being encapsulated inside the polymer matrix along with coumarin. Similar reason was also given in section 4.3.2 where amount of IONPs was increased and increasing NPs size was obtained.

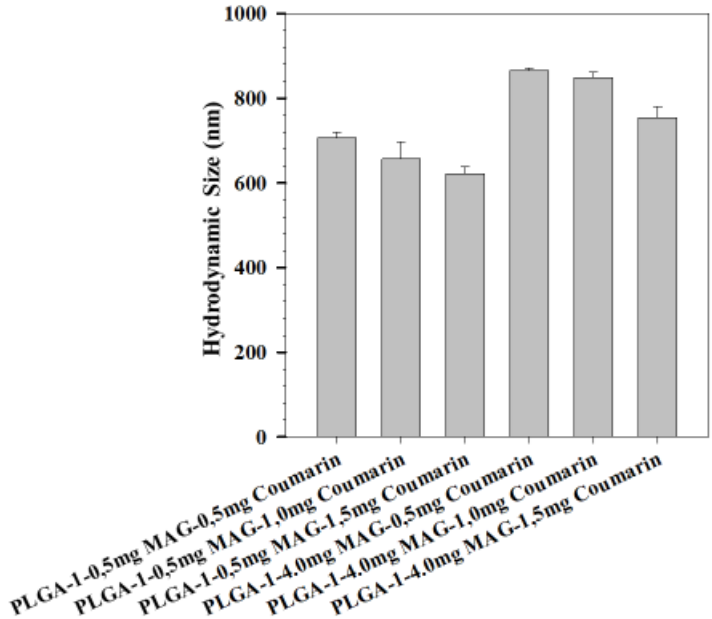

Figure 29: Graphical representation of hydrodynamic size for coumarin loaded PLGA-MAG NPs.

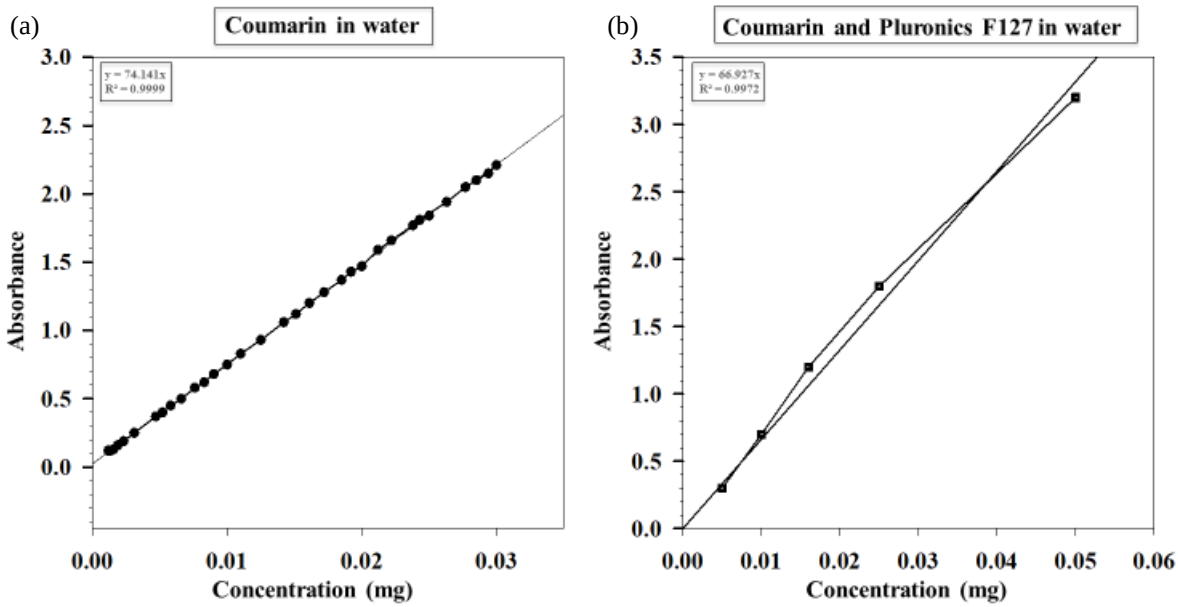

Figure 30: (a) Coumarin calibration curve obtained by UV-Vis in water at 277 nm wavelength and (b) Coumarin + Pluronics F127 calibration curve in water obtained from UV-Vis at 277 nm wavelength.

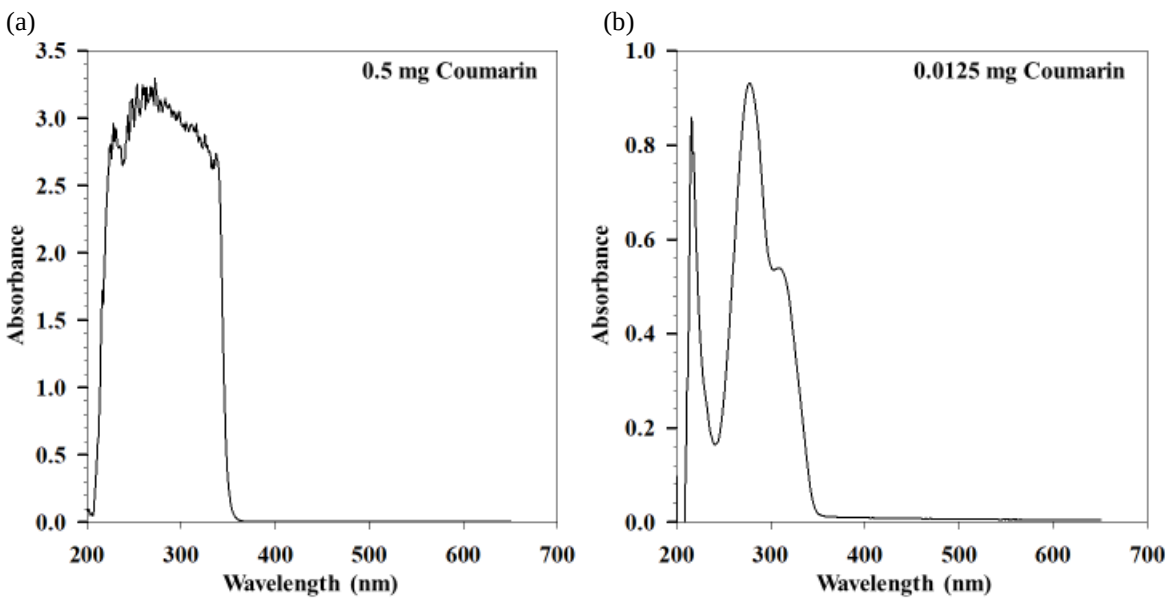

Figure 31: (a) UV-Vis spectra for 0.5 mg coumarin in water and (b) UV-Vis spectra for 0.0125 mg coumarin in water.

Table 8: Drug loading efficiencies at three different coumarin concentrations and two different IONPs concentrations used.

NPs	0.5-MAG-0.5	0.5-MAG-1.0	0.5-MAG-1.5	4.0-MAG-0.5 Coumarin	4.0-MAG-1.0 Coumarin	4.0-MAG-1.5 Coumarin
Wavelength (nm)	277	277	277	277	277	277
UV-Vis Absorbance	0.306	0.401	0.528	0.329	0.401	0.554
Drug amount estimated from	0.004	0.005	0.007	0.004	0.005	0.007
Drug in Supernatant (mg)	0.09	0.12	0.15	0.10	0.12	0.16
Drug loaded (mg)	0.41	0.88	1.35	0.40	0.88	1.34
Drug loading efficiency %	82	88	90	81	88	89

5. Conclusion

In this study, the hydrophilic IONPs were successfully encapsulated using PLGA with different molecular weights. According to statistical design of experiment, it is found that the molecular weight of PLGA and amount of IONPs are the most important parameters that effect the size of NPs significantly.

In synthesis of IONPs by co-precipitation, IONPs with size of 15 ± 2 nm were synthesized successfully synthesized. Bare PLGA NPs were also synthesized and the size was obtained in the range of 80-110 nm. Following that, successful attempt was made to encapsulate IONPs into PLGA NPs. The process of obtaining PLGA-MAG NPs was optimized by conducting preliminary studies of optimization. These studies included the magnetic separation time, mixing of IONPs with PLGA/DMSO mixture, IONPs batch stock concentration effect on size and methodology to identify various populations. Hence, from these studies, all the important parameters that can influence the NPs size were optimized. Also, it was identified that nanoprecipitation process needs further optimization in order to only obtain the PLGA-MAG NPs.

The two statistical designs of experiments also gave satisfactory results for the variation of different parameters that effect the size. This helped us in understanding that molecular weight of PLGA and amount of IONPs can greatly affect the size of NPs. Hence, these parameters must be optimized in order to get NPs of desired size. A hypothesis for encapsulation of IONPs into PLGA NPs was also proposed. It was hypothesized that IONPs and PLGA NPs have Van der Waals interactions. Due to these interactions, when polymer starts to precipitate after coming in contact with the non-solvent phase, the IONPs are entrapped inside the polymer matrix. Hence, they are encapsulated and form PLGA-MAG NPs. However, a complete study is required to understand the interactions between the IONPs and PLGA.

In the last section, coumarin was successfully loaded in PLGA NPs and PLGA-MAG NPs with drug loading efficiencies of 91 and 90 % respectively at the highest concentration of drug used. All the studies presented in this report have not been reported so far in the present literature.

6. Future Work

In future it would be interesting to study the interactions of IONPs with PLGA using various characterization techniques such as Raman spectral analysis and isothermal titration calorimetry. These techniques can provide information about how IONPs interact with PLGA.

Monodisperse IONPs can be synthesized by thermal decomposition process and their encapsulation in PLGA can be studied. In order to compare the size difference for different type of IONPs.

In this report, it was challenging to see the PLGA-MAG NPs by HR-TEM because of the staining issues. Hence, a protocol must be developed for staining these PLGA-MAG NPs and to visualize them using different microscopy techniques.

Although, most of the parameters in this report were optimized but still there is a need of optimization of encapsulation process of IONPs in PLGA NPs. In future, optimization studies must be conducted in order to avoid the obtainment of different populations after PLGA-MAG NPs synthesis.

Since, in this report, hydrophobic drug i.e., coumarin was loaded into PLGA NPs and PLGA-MAG NPs. An attempt to encapsulate drug hydrophilic drugs using nanoprecipitation must be made.

7. Reference

1. Marghussian, V., *Nano-Glass Ceramics: Processing, Properties and Applications*. 2015: William Andrew.
2. Bohara, R.A., N.D. Thorat, and S.H. Pawar, *Role of functionalization: strategies to explore potential nano-bio applications of magnetic nanoparticles.* RSC advances, 2016. **6**(50): p. 43989-44012.
3. Kurlyandskaya, G.V., et al., *Water-Based suspensions of iron oxide nanoparticles with electrostatic or steric stabilization by chitosan: Fabrication, characterization and biocompatibility.* Sensors, 2017. **17**(11): p. 2605.
4. Palma, S.I., et al., *Effects of phase transfer ligands on monodisperse iron oxide magnetic nanoparticles.* Journal of colloid and interface science, 2015. **437**: p. 147-155.
5. Gonzales, M. and K.M. Krishnan, *Phase transfer of highly monodisperse iron oxide nanocrystals with Pluronic F127 for biomedical applications.* Journal of Magnetism and Magnetic Materials, 2007. **311**(1): p. 59-62.
6. Wang, Y., et al., *"Pulling" nanoparticles into water: phase transfer of oleic acid stabilized monodisperse nanoparticles into aqueous solutions of α-cyclodextrin.* Nano Letters, 2003. **3**(11): p. 1555-1559.
7. Anbarasu, M., et al., *Synthesis and characterization of polyethylene glycol (PEG) coated Fe3O4 nanoparticles by chemical co-precipitation method for biomedical applications.* Spectrochimica Acta Part A: Molecular and Biomolecular Spectroscopy, 2015. **135**: p. 536-539.
8. Shete, P., et al., *Magnetic chitosan nanocomposite for hyperthermia therapy application: Preparation, characterization and in vitro experiments.* Applied Surface Science, 2014. **288**: p. 149-157.
9. Etheridge, M.L., et al., *Accounting for biological aggregation in heating and imaging of magnetic nanoparticles.* Technology, 2014. **2**(03): p. 214-228.
10. Rossell, D.W., *Exploding Teeth, Unbreakable Sheets and Continuous Casting: Nitrocellulose from Gun-Cotton to Early Cinema*. 2002, Fédération Internationale des Archives du Film.

11. Gilding, D. and A. Reed, *Biodegradable polymers for use in surgery—polyglycolic/poly (actic acid) homo-and copolymers: 1.* Polymer, 1979. **20**(12): p. 1459-1464.
12. Kulkarni, R., et al., *Polylactic acid for surgical implants.* Archives of surgery, 1966. **93**(5): p. 839-843.
13. Jackanicz, T.M., et al., *Polylactic acid as a biodegradable carrier for contraceptive steroids.* Contraception, 1973. **8**(3): p. 227-234.
14. Bonelli, P., et al., *Ibuprofen delivered by poly (lactic-co-glycolic acid)(PLGA) nanoparticles to human gastric cancer cells exerts antiproliferative activity at very low concentrations.* International journal of nanomedicine, 2012. **7**: p. 5683.
15. Ebrahimian, M., et al., *Co-delivery of doxorubicin encapsulated PLGA nanoparticles and Bcl-xL shRNA using alkyl-modified PEI into breast cancer cells.* Applied biochemistry and biotechnology, 2017. **183**(1): p. 126-136.
16. Aina, A., et al., *Monitoring model drug microencapsulation in PLGA scaffolds using X-ray powder diffraction.* Saudi Pharmaceutical Journal, 2016. **24**(2): p. 227-231.
17. Hines, D.J. and D.L. Kaplan, *Poly (lactic-co-glycolic) acid–controlled-release systems: experimental and modeling insights.* Critical Reviews™ in Therapeutic Drug Carrier Systems, 2013. **30**(3).
18. Hoshyar, N., et al., *The effect of nanoparticle size on in vivo pharmacokinetics and cellular interaction.* Nanomedicine, 2016. **11**(6): p. 673-692.
19. Gentile, P., et al., *An overview of poly (lactic-co-glycolic) acid (PLGA)-based biomaterials for bone tissue engineering.* International journal of molecular sciences, 2014. **15**(3): p. 3640-3659.
20. Wu, X.S. and N. Wang, *Synthesis, characterization, biodegradation, and drug delivery application of biodegradable lactic/glycolic acid polymers. Part II: biodegradation.* Journal of Biomaterials Science, Polymer Edition, 2001. **12**(1): p. 21-34.
21. Swider, E., et al., *Customizing poly (lactic-co-glycolic acid) particles for biomedical applications.* Acta biomaterialia, 2018. **73**: p. 38-51.
22. Vert, M., J. Mauduit, and S. Li, *Biodegradation of PLA/GA polymers: increasing complexity.* Biomaterials, 1994. **15**(15): p. 1209-1213.

23. Makadia, H.K. and S.J. Siegel, *Poly lactic-co-glycolic acid (PLGA) as biodegradable controlled drug delivery carrier.* Polymers, 2011. **3**(3): p. 1377-1397.
24. Zhou, S., et al., *Synthesis and characterization of biodegradable low molecular weight aliphatic polyesters and their use in protein-delivery systems.* Journal of applied polymer science, 2004. **91**(3): p. 1848-1856.
25. Ajioka, M., et al., *Aliphatic polyesters and their copolymers synthesized through direct condensation polymerization.* Polymer Degradation and Stability, 1998. **59**(1-3): p. 137-143.
26. Avgoustakis, K., *Polylactic-co-glycolic acid (PLGA).* Encyclopedia of biomaterials and biomedical engineering, 2005. **1**(1): p. 1-11.
27. Zhou, Z., X. Liu, and L. Liu, *Preparation and biocompatibility of poly (L-lactide-co-glycolide) scaffold materials for nerve conduits.* Designed Monomers and Polymers, 2008. **11**(5): p. 447-456.
28. Kricheldorf, H.R., C. Boettcher, and K.-U. Tönnes, *Polylactones: 23. Polymerization of racemic and mesod, l-lactide with various organotin catalysts—Stereochemical aspects.* Polymer, 1992. **33**(13): p. 2817-2824.
29. Duval, C., C. Nouvel, and J.L. Six, *Is bismuth subsalicylate an effective nontoxic catalyst for plga synthesis?* Journal of Polymer Science Part A: Polymer Chemistry, 2014. **52**(8): p. 1130-1138.
30. Avgoustakis, K. and J. Nixon, *Biodegradable controlled release tablets 1: preparative variables affecting the properties of poly (lactide-co-glycolide) copolymers as matrix forming material.* International journal of pharmaceutics, 1991. **70**(1-2): p. 77-85.
31. Wischke, C. and S.P. Schwendeman, *Principles of encapsulating hydrophobic drugs in PLA/PLGA microparticles.* International Journal of pharmaceutics, 2008. **364**(2): p. 298-327.
32. Pan, J. and S.-S. Feng, *Targeted delivery of paclitaxel using folate-decorated poly (lactide)–vitamin E TPGS nanoparticles.* Biomaterials, 2008. **29**(17): p. 2663-2672.
33. Manchanda, R., et al., *Preparation and characterization of a polymeric (PLGA) nanoparticulate drug delivery system with simultaneous incorporation of chemotherapeutic and thermo-optical agents.* Colloids and Surfaces B: Biointerfaces, 2010. **75**(1): p. 260-267.

34. Keum, C.-G., et al., *Practical preparation procedures for docetaxel-loaded nanoparticles using polylactic acid-co-glycolic acid.* International journal of nanomedicine, 2011. **6**: p. 2225.
35. Zhang, H., J. Bei, and S. Wang, *Multi-morphological biodegradable PLGE nanoparticles and their drug release behavior.* Biomaterials, 2009. **30**(1): p. 100-107.
36. Bodmeier, R. and J.W. McGinity, *Polylactic acid microspheres containing quinidine base and quinidine sulphate prepared by the solvent evaporation technique. II. Some process parameters influencing the preparation and properties of microspheres.* Journal of microencapsulation, 1987. **4**(4): p. 289-297.
37. Wang, Y., et al., *Manufacturing techniques and surface engineering of polymer based nanoparticles for targeted drug delivery to cancer.* Nanomaterials, 2016. **6**(2): p. 26.
38. Giri, T.K., et al., *Prospects of pharmaceuticals and biopharmaceuticals loaded microparticles prepared by double emulsion technique for controlled delivery.* Saudi Pharmaceutical Journal, 2013. **21**(2): p. 125-141.
39. Uchida, T., et al., *Optimization of preparative conditions for polylactide (PLA) microspheres containing ovalbumin.* Chemical and pharmaceutical bulletin, 1995. **43**(9): p. 1569-1573.
40. Lee, B.K., Y. Yun, and K. Park, *PLA micro-and nano-particles.* Advanced drug delivery reviews, 2016. **107**: p. 176-191.
41. Allouche, J. and R. Brayner, *Nanomaterials: A Danger or a Promise.* Brayner, R., Fiévet, F., Coradin, T., Eds, 2013: p. 27.
42. Zabihi, F., et al., *High yield and high loading preparation of curcumin–PLGA nanoparticles using a modified supercritical antisolvent technique.* Industrial & Engineering Chemistry Research, 2014. **53**(15): p. 6569-6574.
43. Reis, C.P., et al., *Nanoencapsulation I. Methods for preparation of drug-loaded polymeric nanoparticles.* Nanomedicine: Nanotechnology, Biology and Medicine, 2006. **2**(1): p. 8-21.
44. Pamujula, S., et al., *Oral delivery of spray dried PLGA/amifostine nanoparticles.* Journal of pharmacy and pharmacology, 2004. **56**(9): p. 1119-1125.
45. Merkulova, M., et al., *PREPARATION OF DRUG-LOADED PLGA NANOPARTICLES BY SPRAY-DRYING USING A BÜCHI SPRAY DRYER B-90.* International Multidisciplinary Scientific GeoConference: SGEM, 2019. **19**(6.1): p. 355-363.

46. Valo, H., et al., *Electrospray encapsulation of hydrophilic and hydrophobic drugs in poly (L-lactic acid) nanoparticles.* Small, 2009. **5**(15): p. 1791-1798.
47. Chiesa, E., et al., *The microfluidic technique and the manufacturing of polysaccharide nanoparticles.* Pharmaceutics, 2018. **10**(4): p. 267.
48. Zhang, L., et al., *Microfluidic methods for fabrication and engineering of nanoparticle drug delivery systems.* ACS Applied Bio Materials, 2019. **3**(1): p. 107-120.
49. Rhee, M., et al., *Synthesis of size-tunable polymeric nanoparticles enabled by 3D hydrodynamic flow focusing in single-layer microchannels.* Advanced Materials, 2011. **23**(12): p. H79-H83.
50. Barreras-Urbina, C.G., et al., *Nano-and micro-particles by nanoprecipitation: Possible application in the food and agricultural industries.* International journal of food properties, 2016. **19**(9): p. 1912-1923.
51. Fessi, H., et al., *Nanocapsule formation by interfacial polymer deposition following solvent displacement.* International journal of pharmaceutics, 1989. **55**(1): p. R1-R4.
52. Salatin, S., et al., *Development of a nanoprecipitation method for the entrapment of a very water soluble drug into Eudragit RL nanoparticles.* Research in pharmaceutical sciences, 2017. **12**(1): p. 1.
53. Quintanar-Guerrero, D., et al., *Preparation techniques and mechanisms of formation of biodegradable nanoparticles from preformed polymers.* Drug development and industrial pharmacy, 1998. **24**(12): p. 1113-1128.
54. Galindo-Rodriguez, S., et al., *Physicochemical parameters associated with nanoparticle formation in the salting-out, emulsification-diffusion, and nanoprecipitation methods.* Pharmaceutical research, 2004. **21**(8): p. 1428-1439.
55. Mora-Huertas, C., H. Fessi, and A. Elaissari, *Influence of process and formulation parameters on the formation of submicron particles by solvent displacement and emulsification–diffusion methods: Critical comparison.* Advances in colloid and interface science, 2011. **163**(2): p. 90-122.
56. Ostrovsky, M.V. and R.M. Ostrovsky, *Dynamic interfacial tension in binary systems and spontaneous pulsation of individual drops by their dissolution.* Journal of Colloid and Interface Science, 1983. **93**(2): p. 392-401.

57. Beck-Broichsitter, M., et al., *Preparation of nanoparticles by solvent displacement for drug delivery: a shift in the "ouzo region" upon drug loading.* European Journal of Pharmaceutical Sciences, 2010. **41**(2): p. 244-253.
58. Ganachaud, F. and J.L. Katz, *Nanoparticles and nanocapsules created using the ouzo effect: spontaneous emulsification as an alternative to ultrasonic and high-shear devices.* ChemPhysChem, 2005. **6**(2): p. 209-216.
59. Aubry, J., et al., *Nanoprecipitation of polymethylmethacrylate by solvent shifting: 1. Boundaries.* Langmuir, 2009. **25**(4): p. 1970-1979.
60. Stainmesse, S., et al., *Formation and stabilization of a biodegradable polymeric colloidal suspension of nanoparticles.* Colloid and Polymer Science, 1995. **273**(5): p. 505-511.
61. Hernández-Giottonini, K.Y., et al., *PLGA nanoparticle preparations by emulsification and nanoprecipitation techniques: effects of formulation parameters.* RSC Advances, 2020. **10**(8): p. 4218-4231.
62. Rezvantalab, S., et al., *PLGA-Based Nanoparticles in Cancer Treatment.* Frontiers in pharmacology, 2018. **9**: p. 1260-1260.
63. Madani, F., et al., *Investigation of Effective Parameters on Size of Paclitaxel Loaded PLGA Nanoparticles.* Advanced pharmaceutical bulletin, 2018. **8**(1): p. 77-84.
64. Budhian, A., S.J. Siegel, and K.I. Winey, *Haloperidol-loaded PLGA nanoparticles: Systematic study of particle size and drug content.* International Journal of Pharmaceutics, 2007. **336**(2): p. 367-375.
65. Lince, F., D.L. Marchisio, and A.A. Barresi, *Strategies to control the particle size distribution of poly-ε-caprolactone nanoparticles for pharmaceutical applications.* Journal of Colloid and Interface Science, 2008. **322**(2): p. 505-515.
66. Badri, W., et al., *Elaboration of nanoparticles containing indomethacin: Argan oil for transdermal local and cosmetic application.* Journal of Nanomaterials, 2015. **2015**.
67. Huang, W. and C. Zhang, *Tuning the size of poly (lactic-co-glycolic acid)(PLGA) nanoparticles fabricated by nanoprecipitation.* Biotechnology journal, 2018. **13**(1): p. 1700203.
68. Sahana, D., et al., *PLGA nanoparticles for oral delivery of hydrophobic drugs: influence of organic solvent on nanoparticle*

formation and release behavior in vitro and in vivo using estradiol as a model drug. Journal of pharmaceutical sciences, 2008. **97**(4): p. 1530-1542.

69. Öztürk, A.A., E. Yenilmez, and M.G. Özarda, *Clarithromycin-loaded poly (lactic-co-glycolic acid)(PLGA) nanoparticles for oral administration: effect of polymer molecular weight and surface modification with chitosan on formulation, nanoparticle characterization and antibacterial effects.* Polymers, 2019. **11**(10): p. 1632.
70. Martín-Banderas, L., et al., *Cannabinoid derivate-loaded PLGA nanocarriers for oral administration: formulation, characterization, and cytotoxicity studies.* International journal of nanomedicine, 2012. **7**: p. 5793.
71. Cheow, W.S. and K. Hadinoto, *Enhancing encapsulation efficiency of highly water-soluble antibiotic in poly(lactic-co-glycolic acid) nanoparticles: Modifications of standard nanoparticle preparation methods.* Colloids and Surfaces A: Physicochemical and Engineering Aspects, 2010. **370**(1): p. 79-86.
72. Boisvert, A.-A., et al., *Microbial Biofilms in Pulmonary and Critical Care Diseases.* Annals of the American Thoracic Society, 2016. **13**(9): p. 1615-1623.
73. Chourasiya, V., S. Bohrey, and A. Pandey, *Formulation, optimization, characterization and in-vitro drug release kinetics of atenolol loaded PLGA nanoparticles using 33 factorial design for oral delivery.* Materials Discovery, 2016. **5**: p. 1-13.
74. Fonseca, C., S. Simões, and R. Gaspar, *Paclitaxel-loaded PLGA nanoparticles: preparation, physicochemical characterization and in vitro anti-tumoral activity.* Journal of Controlled Release, 2002. **83**(2): p. 273-286.
75. Govender, T., et al., *PLGA nanoparticles prepared by nanoprecipitation: drug loading and release studies of a water soluble drug.* Journal of Controlled Release, 1999. **57**(2): p. 171-185.
76. Tansık, G., A. Yakar, and U. Gündüz, *Tailoring magnetic PLGA nanoparticles suitable for doxorubicin delivery.* Journal of Nanoparticle Research, 2013. **16**(1): p. 2171.
77. Schleich, N., et al., *Dual anticancer drug/superparamagnetic iron oxide-loaded PLGA-based nanoparticles for cancer therapy and magnetic resonance imaging.* International Journal of Pharmaceutics, 2013. **447**(1): p. 94-101.

78. Smith, D.J., *High Resolution Transmission Electron Microscopy*, in *Handbook of Microscopy for Nanotechnology*, N. Yao and Z.L. Wang, Editors. 2005, Springer US: Boston, MA. p. 427-453.
79. Malvern. *MAN 0317*. 2013; Manual of DLS]. Available from: https://www.chem.uci.edu/~dmitryf/manuals/Fundamentals/DLS%20measurement%20principles.pdf.
80. Stetefeld, J., S.A. McKenna, and T.R. Patel, *Dynamic light scattering: a practical guide and applications in biomedical sciences.* Biophys Rev, 2016. **8**(4): p. 409-427.
81. Cheraghipour, E., S. Javadpour, and A.R. Mehdizadeh, *Citrate capped superparamagnetic iron oxide nanoparticles used for hyperthermia therapy.* Journal of Biomedical Science and Engineering, 2012. **Vol.05No.12**: p. 5.
82. Easo, S.L. and P.V. Mohanan, *Dextran stabilized iron oxide nanoparticles: synthesis, characterization and in vitro studies.* Carbohydr Polym, 2013. **92**(1): p. 726-32.
83. Dave, P.N. and L.V. Chopda, *Application of Iron Oxide Nanomaterials for the Removal of Heavy Metals.* Journal of Nanotechnology, 2014. **2014**: p. 398569.
84. Nicolete, R., D.F.d. Santos, and L.H. Faccioli, *The uptake of PLGA micro or nanoparticles by macrophages provokes distinct in vitro inflammatory response.* International Immunopharmacology, 2011. **11**(10): p. 1557-1563.
85. Hernández-Giottonini, K.Y., et al., *PLGA nanoparticle preparations by emulsification and nanoprecipitation techniques: effects of formulation parameters.* RSC Advances, 2020. **10**: p. 4218-4231.
86. Öztürk, A.A., E. Yenilmez, and M.G. Özarda, *Clarithromycin-Loaded Poly (Lactic-co-glycolic Acid) (PLGA) Nanoparticles for Oral Administration: Effect of Polymer Molecular Weight and Surface Modification with Chitosan on Formulation, Nanoparticle Characterization and Antibacterial Effects.* Polymers, 2019. **11**(10): p. 1632.
87. Shkodra-Pula, B., et al., *Effect of surfactant on the size and stability of PLGA nanoparticles encapsulating a protein kinase C inhibitor.* International Journal of Pharmaceutics, 2019. **566**: p. 756-764.
88. Menon, J.U., et al., *Effects of surfactants on the properties of PLGA nanoparticles.* Journal of Biomedical Materials Research Part A, 2012. **100A**(8): p. 1998-2005.

89. Ezzaier, H., et al., *Kinetics of Aggregation and Magnetic Separation of Multicore Iron Oxide Nanoparticles: Effect of the Grafted Layer Thickness.* Nanomaterials (Basel, Switzerland), 2018. **8**(8): p. 623.
90. Xie, H. and J.W. Smith, *Fabrication of PLGA nanoparticles with a fluidic nanoprecipitation system.* Journal of Nanobiotechnology, 2010. **8**(1): p. 18.
91. Hoda, M., et al., *Stabilizers influence drug-polymer interactions and physicochemical properties of disulfiram-loaded poly-lactide-co-glycolide nanoparticles.* Future science OA, 2017. **4**(2): p. FSO263-FSO263.

8. Appendix

A. Graph for population identification methodology (from section 4.2.2)

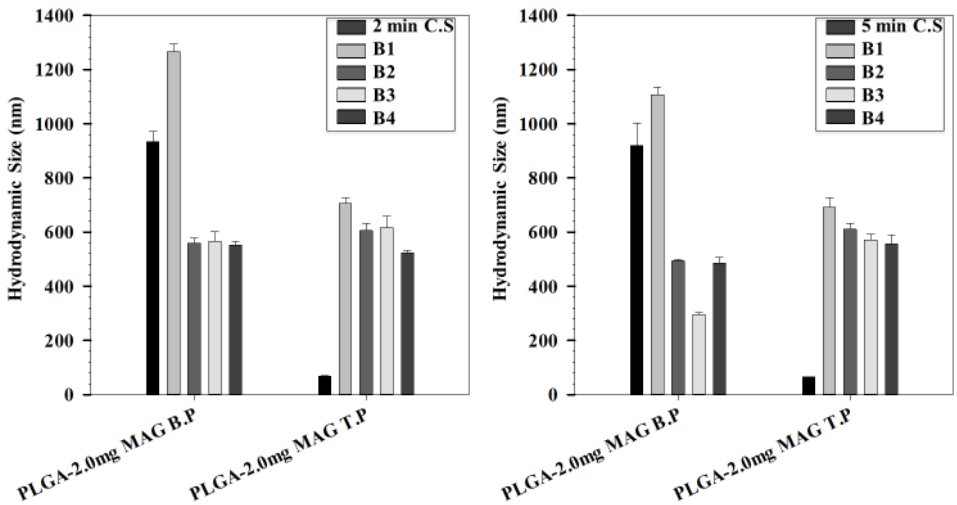

Figure A.1: Graph for 2mg IONPs concentration for identification of different populations.

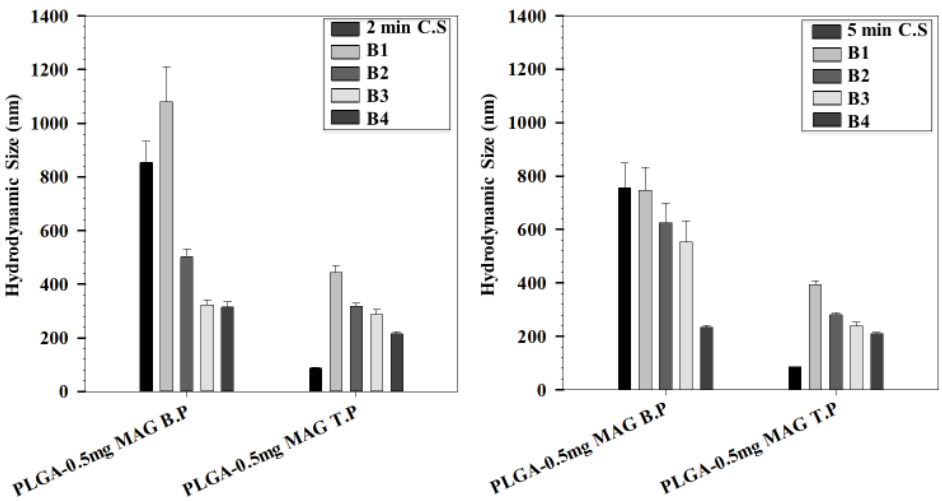

Figure A.2: Graph for 0.5 mg IONPs concentration for identification of different populations.

B. Graph for experimental repeats of different IONPs batch concentrations (from section 4.2.4)

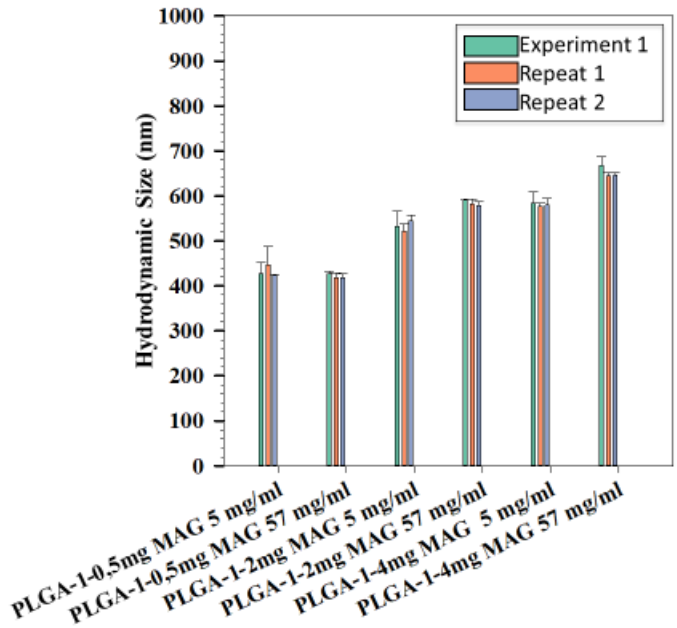

Figure B.1: Graphical representation of three experimental repeats at different IONPs batch concentrations

C. JMP Study Experimental Design

Experiment No.	Aqueous/Organic ratio (v/v)	Injection rate (ml/hr)	Molecular Weight (Da)	Polymer/IONPs ratio (w/w)	Hydrodynamic size (nm)
1	20	4.5	13000	7.5	710.6
2	5	4.5	13000	20	476.8
3	5	13.5	13000	20	457.8
4	20	13.5	13000	20	455.1
5	20	4.5	45000	7.5	347.4
6	5	13.5	13000	7.5	714.8
7	20	4.5	45000	20	321.3
8	5	13.5	45000	7.5	383.1
9	20	13.5	13000	7.5	748.1
10	20	13.5	45000	20	297.7
11	20	4.5	13000	20	300.9
12	5	4.5	13000	7.5	692.4
13	20	13.5	45000	7.5	282.4
14	5	4.5	45000	7.5	330
15	5	13.5	45000	20	239.2
16	5	4.5	45000	20	205

Table C.1: Experimental design for JMP Study 1

Experiment No.	Molecular Weight (Da)	IONPs amount (mg)	Polymer amount (mg)	Hydrodynamic size (nm)
1	31000	2	10	474.8
2	31000	2	30	560.2
3	45000	4	10	373.5
4	31000	4	10	560
5	14000	2	10	461.4
6	45000	4	30	395.5
7	14000	2	20	570.5
8	31000	4	30	679.8
9	14000	0.5	20	409.2
10	31000	2	20	508.2
11	45000	0.5	30	322
12	14000	2	30	650.2
13	14000	4	20	679.2
14	31000	0.5	10	329.8
15	45000	2	30	357.4
16	45000	4	20	345.2
17	45000	0.5	20	323.8
18	31000	0.5	20	394.2
19	45000	2	20	302.9
20	14000	0.5	30	572.1
21	31000	4	20	586.3
22	45000	0.5	10	250.2
23	45000	2	10	280.5
24	14000	4	10	580.4
25	14000	0.5	10	325.1
26	31000	0.5	30	404.5
27	14000	4	30	731.7

Table C.2: Experimental design for JMP Study 2